

**NASA CONTRACTOR
REPORT**

NASA CR-2655



NASA CR-2655

0061507



**COMBUSTION OF HYDROGEN INJECTED
INTO A SUPERSONIC AIRSTREAM
(A GUIDE TO THE HISS COMPUTER PROGRAM)**

LOAN COPY: RETURN TO
AFWL TECHNICAL LIBRARY
KIRTLAND AFB, N. M.

D. F. Dyer, G. Maples, and D. B. Spalding

Prepared by
FLUID MECHANICS AND THERMAL SYSTEMS, INC.
Waverly, Ala. 36879
for Langley Research Center



NATIONAL AERONAUTICS AND SPACE ADMINISTRATION • WASHINGTON, D. C. • MARCH 1976



0061507

1. Report No. NASA CR-2655		2. Government Accession No.		3. Recipient's Catalog No.	
4. Title and Subtitle COMBUSTION OF HYDROGEN INJECTED INTO A SUPERSONIC AIRSTREAM (A GUIDE TO THE HISS COMPUTER PROGRAM)				5. Report Date March 1976	
				6. Performing Organization Code	
7. Author(s) D. F. Dyer, G. Maples, and D. B. Spalding				8. Performing Organization Report No.	
9. Performing Organization Name and Address Fluid Mechanics & Thermal Systems, Inc. Route 2, Box 11 Waverly, AL 36879				10. Work Unit No. 505-05-41-02	
				11. Contract or Grant No.	
12. Sponsoring Agency Name and Address National Aeronautics & Space Administration Washington, DC 20546				13. Type of Report and Period Covered Contractor Report	
				14. Sponsoring Agency Code	
15. Supplementary Notes D. B. Spalding is affiliated with Concentration, Heat & Momentum LTD., 86 Burlington Road, New Malden, Surrey, KT3 4NT, England. Langley technical monitor: Dr. John S. Evans, Jr. Final report					
16. Abstract A computer program based on a finite-difference, implicit numerical integration scheme is described for the prediction of hydrogen injected into a supersonic airstream at an angle ranging from normal to parallel to the airstream main flow direction. Results of calculations for flow and thermal property distributions are compared with "cold flow data" taken by NASA/Langley and show excellent correlation. Typical results for equilibrium combustion are presented and exhibit qualitatively plausible behavior. Computer time required for a given case is approximately one minute on a CDC 7600. A discussion of the assumption of parabolic flow in the injection region is given which demonstrates that improvement in calculation in this region could be obtained by a partially-parabolic procedure which has been developed by FMST consultants. It is concluded that the technique described herein provides an efficient and reliable means for analyzing hydrogen injection into supersonic airstreams and the subsequent combustion.					
17. Key Words (Suggested by Author(s)) Supersonic combustion Turbulent mixing Computer program Normal injection				18. Distribution Statement Unclassified - Unlimited Subject Category 34	
19. Security Classif. (of this report) Unclassified		20. Security Classif. (of this page) Unclassified		21. No. of Pages 76	22. Price* \$4.75



LIST OF CONTENTS

	Page
1. Mathematical Development of HISS	1
2. General Features of HISS	22
3. Invariant Portions of HISS	28
4. Physical Modelling	35
5. Problem Dependent Sections	37
6. Results and Conclusions	39
7. References	54
8. Nomenclature	55
Appendix A	57
Appendix B	71

1. MATHEMATICAL DEVELOPMENT OF HISS

1.0 Introduction

NASA is active in research on supersonic combustion [1-3]. Of particular interest are methods for injecting hydrogen in a supersonic air stream in a manner which achieves effective mixing and a minimum pressure loss. Two arrangements of interest are shown in Figures (1.0-1) and (1.0-2).

This report provides documentation of a finite-difference computer program called HISS (Hydrogen Injection of a Supersonic Stream) which was developed by FMTS under contract to NASA for the exclusive use of NASA; it can be used to predict the flow properties for cases depicted in Figures (1.0-1) and (1.0-2).

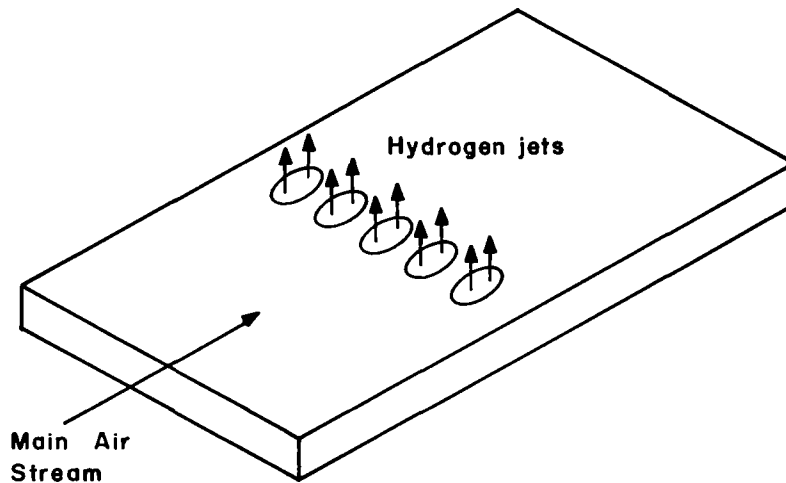


Figure 1.0-1 Normal Injection

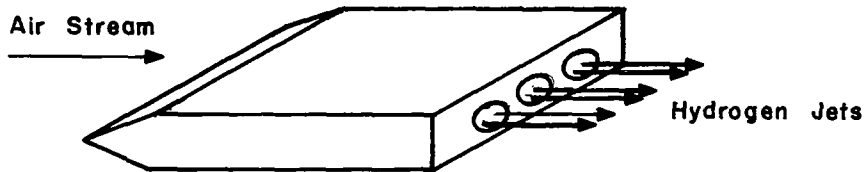


Figure 1.0-2 Parallel Injection

The remaining part of this chapter gives the mathematical equations which are used to model the flow process. The "art" involved in using these equations to develop a finite-difference algorithm for these equations is also described.

1.1 Capabilities and limitations of HISS

HISS is capable of calculating three-dimensional, boundary layer flows which are either external or internal. The geometry considered is flow in a fixed rectangular parallelepiped with "zero-flux" boundary conditions on each side wall, either a free, symmetry or solid wall at the top surface and either a symmetry or wall boundary condition at the bottom surface. It can handle injection of hydrogen ranging from normal to parallel to the main air stream. Five equilibrium reactions are allowed. The main air flow can be either subsonic or supersonic; however, the free stream pressure gradient is considered to be zero.

The flow is considered turbulent and the viscosity is calculated by way of the "k- ϵ " turbulence model described in [4]. Density is calculated via the ideal gas law.

1.2 Numerical method

The numerical method used is described in detail in [5]. A brief discussion will be made to summarize the method.

1.2-1 The differential equation

The general differential equation describing the transport of a fluid property ϕ is expressed in Cartesian coordinates as follows for the fixed volume under consideration:

$$\frac{\partial}{\partial x} (\rho u \phi) + \frac{\partial}{\partial y} (\rho v \phi) + \frac{\partial}{\partial z} (\rho w \phi) = S_{\phi} + \frac{\partial}{\partial x} (\Gamma_{\phi} \frac{\partial \phi}{\partial x}) + \frac{\partial}{\partial y} (\Gamma_{\phi} \frac{\partial \phi}{\partial y}) \quad (1.2-1)$$

where x , y , and z are Cartesian coordinates as illustrated in Figure (1.2-1). ϕ is a general dependent variable.

The governing equations which must be solved are: continuity, momentum equations for each coordinate direction, the energy equation, an equation expressing conservation of total hydrogen and two differential equations for turbulence properties. These equations allow calculations of eight dependent variables, namely u , v , w , p , f , \bar{h} , k and ϵ . All of these equations except continuity have the form of equation (1.2-1) and the respective source terms and transport coefficients are given in Table (1.2-1). The calculation of pressure is described in Section 1.5.

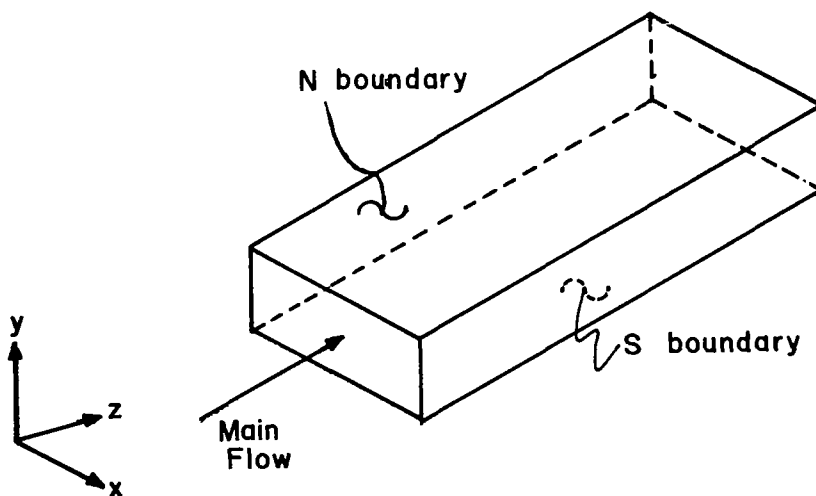


Figure 1.2-1 Coordinate Systems

For these variables, the appropriate transport and source terms are given in Table (1.2-1).

ϕ	Γ_{ϕ}	S_{ϕ}
u	μ_{eff}	$\frac{\partial}{\partial x} (\mu_{\text{eff}} \frac{\partial u}{\partial x}) - \frac{\partial p}{\partial x} + \frac{\partial}{\partial y} (\mu_{\text{eff}} \frac{\partial v}{\partial x})$
v	μ_{eff}	$\frac{\partial}{\partial y} (\mu_{\text{eff}} \frac{\partial v}{\partial y}) - \frac{\partial p}{\partial y} + \frac{\partial}{\partial x} (\mu_{\text{eff}} \frac{\partial u}{\partial y})$
w	μ_{eff}	See Section 1.7
k	$\frac{\mu_t}{\sigma_{t,k}} + \frac{\mu}{\sigma_k}$	$\mu_t \left\{ 2 \left[\left(\frac{\partial u}{\partial x} \right)^2 + \left(\frac{\partial v}{\partial y} \right)^2 \right] + \left(\frac{\partial w}{\partial x} \right)^2 + \left(\frac{\partial w}{\partial y} \right)^2 + \left[\frac{\partial v}{\partial x} + \frac{\partial u}{\partial y} \right]^2 \right\} - \rho \epsilon$
ϵ	$\frac{\mu_{t,\epsilon}}{\sigma_{t,\epsilon}} + \frac{\mu}{\sigma_{\epsilon}}$	$C_1 \frac{\epsilon}{k} \mu_t \left\{ 2 \left[\left(\frac{\partial u}{\partial x} \right)^2 + \left(\frac{\partial v}{\partial y} \right)^2 \right] + \left(\frac{\partial w}{\partial x} \right)^2 + \left(\frac{\partial w}{\partial y} \right)^2 + \left[\frac{\partial v}{\partial x} + \frac{\partial u}{\partial y} \right]^2 \right\} - C_2 \frac{\rho \epsilon^2}{k}$
\bar{h}	$\frac{\mu_t}{\sigma_{t,h}} + \frac{\mu}{\sigma_h}$	$\frac{\partial}{\partial y} \left[\frac{\mu_{\text{eff}}}{\sigma_{\text{eff},\bar{h}}} (\sigma_{\text{eff},\bar{h}} - 1) \frac{\partial w^2/2}{\partial y} \right] + \frac{\partial}{\partial x} \left[\frac{\mu_{\text{eff}}}{\sigma_{\text{eff},\bar{h}}} (\sigma_{\text{eff},\bar{h}} - 1) \frac{\partial w^2/2}{\partial x} \right]$
f	$\frac{\mu_t}{\sigma_{t,f}} + \frac{\mu}{\sigma_f}$	0

Table (1.2-1)

Values for the laminar Prandtl number, σ , and the turbulent Prandtl number $\sigma_{t,\phi}$ along with C_1 and C_2 required in the source term of the k and ϵ equations are given in Table (1.2-2). Also given are

ϕ	$\sigma_{\text{eff},\phi}$	σ
k	1.0	.7
ϵ	1.3	.7
h	.9	.7
f	.9	.7

K	E	C_D	C_1	C_2
.42	9.0	.09	1.44	1.92

Table (1.2-2)

K and E which are constants required in the law-of-the-wall formulation described in section 1.6-4 and the constant C_D used to obtain the dissipation length scale in equation 1.3-2.

1.3 Auxiliary information

In addition to the partial differential equations the complete specification of the problem requires provision of auxiliary information of three types: boundary conditions, physical hypotheses which permit the calculation of diffusion coefficients as well as sources and sinks of each variable, and certain relationships among the thermodynamic and transport properties required to describe the flow.

1.3-1 Boundary conditions

For each of the seven variables listed in Table (1.2-1), values must be specified in the $z = 0$ plane. In addition, boundary conditions along the N and S surface [see Figure (1.2-1)] must be specified for each of these variables. These boundary conditions can be specified

as the value of the variable ϕ or the flux of ϕ through the surface. A detailed discussion of boundary conditions is given in Section 1.6.

1.3-2 Physical hypotheses

The gas density is calculated by the ideal gas law. Details are given in Section 1.7 since special procedures are required to treat mixed subsonic-supersonic flow.

The laminar viscosity is calculated by the formulas presented on page 58 of reference [6] and will not be repeated here.

The turbulent viscosity is calculated by solving conservation equations for the kinetic energy of turbulent fluctuating motion, k , and the energy dissipation rate, ϵ . The turbulent viscosity is then given by:

$$\mu_t = \rho k^{1/2} \ell \quad (1.3-1)$$

where ℓ is a dissipation length scale which can be determined from the equation for ϵ , i.e.:

$$\ell = \frac{C_D k^{3/2}}{\epsilon} \quad (1.3-2)$$

Equations (1.3-1) and (1.3-2) are the basis by which the effective turbulent viscosity is calculated by the k - ϵ model.

1.3-3 Thermodynamic and transport relationships

In order to calculate properties such as laminar viscosity or temperature, it is necessary to know the mass fraction of each chemical specie present at a given location. Thermodynamic equilibrium is assumed so that from the local temperature, pressure, and element fractions the specie mass fraction distribution is calculated. This technique was developed in this work and is reported in detail in Appendix A.

Another important relationship is between the stagnation enthalpy and temperature. This relationship is:

$$\bar{h} = \sum m_{fi} h_i^o + \frac{u^2 + v^2 + w^2}{2} + C_p (T - T_{ref})$$

where C_p is the mixture specific heat and T_{ref} is the reference temperature for which the specie enthalpy of formation, h_i^o , is based. For this work $T_{ref} = 0^\circ\text{K}$. Note that C_p is defined by:

$$C_p \equiv \frac{1}{T - T_{ref}} \int_{T_{ref}}^T C_p dT = \frac{h - h_{ref}}{T - T_{ref}}$$

where h is the sensible enthalpy at the temperature T . Therefore, the definition takes into account the variation of specific heat with temperature.

The density is assumed to vary according to the ideal gas law, namely:

$$\rho = \frac{pW}{RT}$$

1.4 The discretization procedure

The finite-difference equivalents of the differential equations are obtained by integrating the latter over the control volumes which surround the nodes of a grid system. For purposes of this integration, the dependent variables are presumed to vary in a prescribed manner between grid nodes; details of this are available in Patankar and Spalding [5].

1.4-1 The grid system

The grid system used is indicated in Figure (1.4-1). It consists of a system of orthogonal intersecting grid lines in the x - y plane corresponding to a constant value of z .

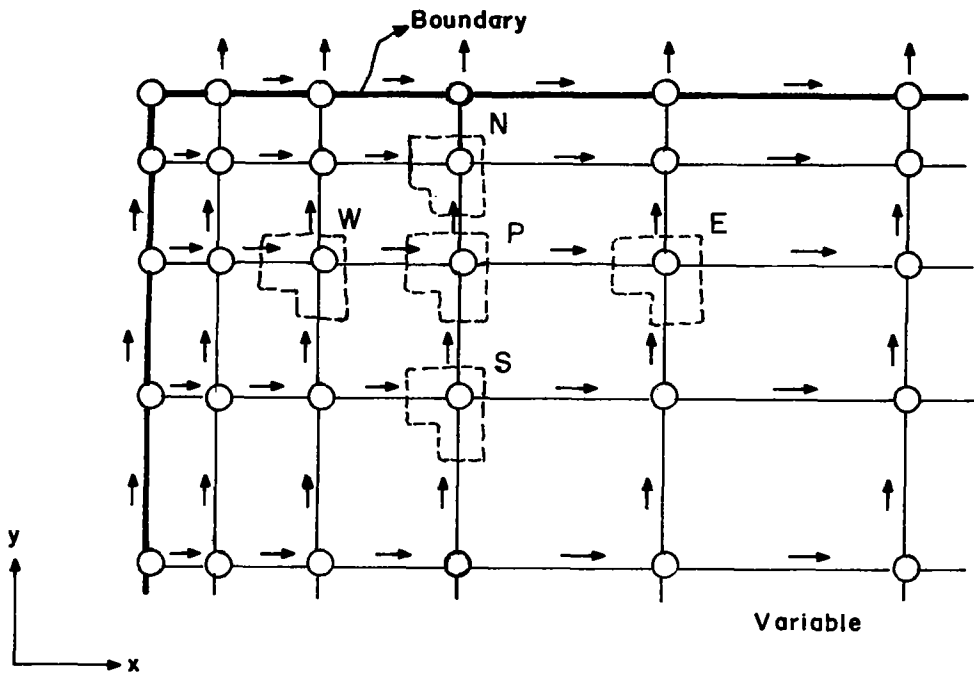


Figure 1.4-1 Grid System

1.4-2 Storage locations

Figure (1.4-1) also indicates the fact that the u and v velocity components are located at points in the grid regularly displaced from the points where all other variables are stored. The boomerang-shaped envelopes enclose the triads of points denoted by the single letter N, S, E, W or P, and represent a unique computer storage location.

1.4-3 Control volumes

The control volume surrounding each grid node P, is indicated by dashed lines in Figure (1.4-2), and is termed the main control volume. Control volumes appropriate to the u and v velocity components are "stag-

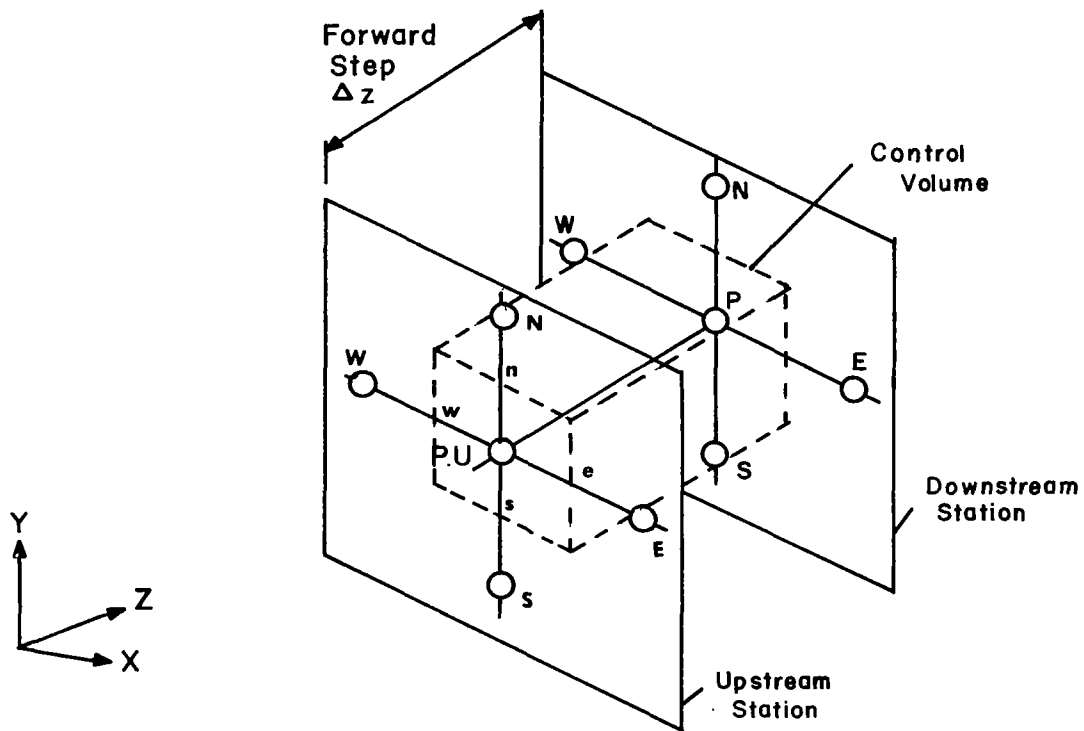


Figure 1.4-2 Main Control Volume

gered" from such main control volumes; the faces of the former being arranged to pass through grid nodes where pressures are stored.

The control volumes corresponding to the near-boundary velocities, v in the case of N and S boundaries and u in the case of E and W boundaries, are arranged to be somewhat larger than their size in the rest of the calculation domain. Figure (1.4-3) illustrates this point. The near-boundary main control volumes remain unchanged.

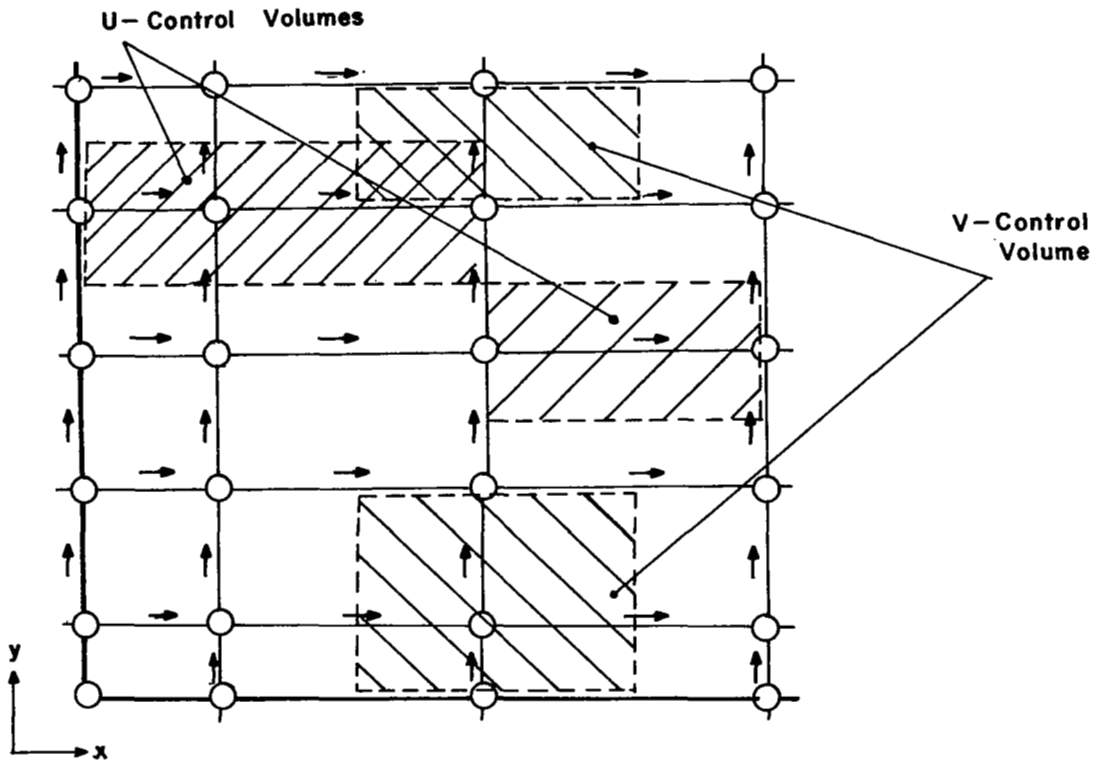


Figure 1.4-3 Near Boundary Velocity Control Volume

1.4-4 The general discretized equation

The general discretized equation is obtained by integrating equation (1.2-1) over the control volume surrounding each grid node. Such an integration is performed after making assumptions about the manner in which the variable ϕ is distributed between grid nodes. All

dependent variables are presumed so to vary, linearly in the x and y directions and in castellated fashion along the z direction. The result of the above-mentioned operation is an algebraic equation for each grid location. This algebraic equation now represents the discretized form of the balance equation for ϕ , over the control volume surrounding the grid location. The balance equation is expressed simply as:

$$\begin{aligned}
 & \left[F_D \phi_P - F_U \phi_{P,U} \right] + \left[L_n^y (\phi_N + \phi_P) - L_s^y (\phi_P + \phi_S) \right] \\
 & + \left[L_e^x (\phi_E + \phi_P) - L_w^x (\phi_P + \phi_W) \right] = S_P^\phi \\
 & + \left[T_n^y (\phi_N - \phi_P) - T_s^y (\phi_P - \phi_S) \right] + \left[T_e^x (\phi_E - \phi_P) - T_w^x (\phi_P - \phi_W) \right]
 \end{aligned} \tag{1.4-1}$$

where the L's represent convective contributions, T's the diffusive and S the source (and/or sink) contribution to the balance of ϕ . The location of points e, w, n, s, E, W, N, S is given in Figure 1.4-2. These coefficients are defined as follows:

$$F_U = [\rho w]_{P,U} \Delta x \Delta y \tag{a}$$

$$L_n^y = [\rho v]_n \frac{\Delta x \Delta z}{2} \quad L_s^y = [\rho v]_s \frac{\Delta x \Delta z}{2} \tag{b}$$

$$L_e^x = [\rho u]_e \frac{\Delta y \Delta z}{2} \quad L_w^x = [\rho u]_w \frac{\Delta y \Delta z}{2} \tag{c}$$

(1.4-2)

$$F_D = F_U - 2L_e^x + 2L_w^x - 2L_n^y + 2L_s^y \tag{d}$$

$$T_e^x = \Gamma_{\phi,e} \frac{\Delta y \Delta z}{\delta x_e} \quad T_w^x = \Gamma_{\phi,w} \frac{\Delta y \Delta z}{\delta x_w} \tag{e}$$

$$T_s^y = \Gamma_{\phi,s} \frac{\Delta x \Delta z}{\delta y_s} \quad T_n^y = \Gamma_{\phi,n} \frac{\Delta x \Delta z}{\delta y_n} \tag{f}$$

$$S_P^\phi = S_{\phi,P} \Delta x \Delta y \Delta z \quad (g)$$

$$\delta x_e = x_P - x_E \quad \delta x_w = x_W - x_P \quad (h)$$

$$\delta y_s = y_P - y_S \quad \delta y_n = y_N - y_P \quad (i) \quad (1.4-2)$$

$$\Delta x = |x_e - x_w| \quad (j)$$

$$\Delta y = |y_n - y_s| \quad (k)$$

where the subscripts e, w, n, s, E, W, N, S indicate location defined in Figure 1.4-2, Δz is the forward step size and S^ϕ is always expressed in linearized form as:

$$S_P^\phi = S_U + S_P \phi_P \quad (1.4-3)$$

On re-arranging the terms of equation (1.4-1), we have:

$$\phi_P = A_N \phi_N + A_S \phi_S + A_E \phi_E + A_W \phi_W + B \quad (1.4-4)$$

where the coefficients A_i' are defined as follows:

$$A_E' = (T_e^X - L_e^X)/A_P' \quad (a)$$

(1.4-5)

$$A_W' = (T_w^X + L_w^X)/A_P' \quad (b)$$

$$A_N^i = (T_n^y - L_n^y) / A_p^i \quad (c)$$

$$A_S^i = (T_s^y + L_s^y) / A_p^i \quad (d) \quad (1.4-5)$$

$$B = [(S_U + S_p \phi_p) + F_U \phi_{p,U}] / A_p^i \quad (e)$$

$$A_p^i = T_n^y + T_s^y + T_e^x + T_w^x - L_n^y + L_s^y - L_e^x + L_w^x + F_U - S_p \quad (f)$$

It is possible for the ratio of convective contribution L_m^n to the coefficient A_M^i to become large on occasions resulting in the coefficient becoming negative. Were equation (1.4-4) to be solved with negative coefficients, physically implausible results would ensue. To overcome such a possibility, a hybrid scheme, well-known as the high-lateral-flux-modification (see Reference [5]) is introduced. This scheme consists of replacing all the coefficients of the form T_m^n by \bar{T}_m^n as follows:

$$\bar{T}_m^n = T_m^n + |L_m^n| + |T_m^n| - |L_m^n| \quad (1.4-6)$$

where, $|L|$ signifies the modulus of L .

1.5 The computational algorithm

The computational algorithm embodied in HISS, is the SIMPLE (for Semi-Implicit Method for Pressure-Linked Equations) scheme reported in reference [5]*. In brief, this scheme is described as follows.

Approximate forms of discretized momentum equations are first solved with a guessed-at pressure-field. The resulting "starred" velocity field is used in conjunction with the discretized continuity equation to arrive at a distribution of "pressure-corrections," p' . These pressure-corrections are then used in correcting the pressure and velocity fields simultaneously. The corrected velocity fields are subsequently used in solving the discretized forms of all other equations.

* Reference [5] describes an incompressible solution. The algorithm used in HISS has been modified to handle compressible flow as described in Section 1.7.

Solutions to the algebraic equations themselves are obtained by the use of standard tri-diagonal matrix algorithm (TDMA).

1.6 Boundary conditions

1.6-1 General policy

The HISS program requires the specification of boundary conditions on the N and S boundaries. The boundaries on each side are fixed as "zero flux" boundaries. A clear distinction is made, for all dependent variables, between boundary values and values internal to the domain. The main machinery of the program leaves the boundary values unchanged, although it uses them in determining the internal values. Thus, the procedure is so structured that it nominally solves the fixed-boundary-value problem. When boundary values are not known, however, appropriate modifications are devised which permit the single structure to be used. The following sections describe such modifications.

In general, boundary condition information can be supplied to the numerical calculation procedure in one of four ways. The boundary values of the dependent variables themselves can be modified; or the values of r at the boundary nodes can be suitably adjusted. Alternatively, the source terms for the near-boundary control volumes or the finite-difference coefficients themselves can be suitably modified. HISS is equipped with source-term modification practices.

1.6-2 Boundary conditions for transport equations

Fixed Boundary values

This is the simplest case and the user is merely required to supply the correct boundary values at the start of the calculation procedure; or else, if the 'fixed' boundary conditions vary in any arbitrarily specified manner along the z direction, account can be taken of such variations by suitably updating the boundary value of the appropriate variable.

Fixed gradients at boundaries

When the boundary value of a dependent variable is unknown but the normal gradient or the flux of the variable at the boundary is given, the following practice is adopted. The coefficient of the finite-difference equations connecting the boundary node to an internal node is arranged to

be zero. The boundary flux is then supplied through the source term for the internal node. A common example of this is in the treatment of planes of symmetry. The only action taken here is to set the appropriate finite-difference coefficient to zero.

Retrieval of unknown boundary values

In situations where boundary values of dependent variables are unknown and the boundary coefficient has been set to zero, the value of the dependent variable in the computer register corresponding to the boundary node has no significance. (The wall condition is then represented by the value at the node nearest the wall). In this program no action is taken to modify it so that the initial value of the dependent variable will continue to prevail in such registers.

1.6-3 Boundary conditions for the pressure-correction equation

Unlike the finite-difference equations for a general variable ϕ , the pressure correction equation is programmed with the presumption that all gradients of p' normal to boundaries are zero at the boundaries themselves. The pressure-difference coefficients D^u , D^v and D^w are initialized to zero over the entire calculation domain and remain at this value for the boundary nodes.

1.6-4 Wall functions

The expressions for Γ appropriate to turbulent flow are not strictly valid in the vicinity of wall boundaries to the flow, where laminar viscosity plays an important role. If the near-boundary grid nodes are sufficiently far away from walls, the turbulent viscosity can continue to be used for internal grid nodes. However, means must be provided for the calculation of the correct shear stresses as well as fluxes of other dependent variables at the wall boundaries. Provisions for such calculations are made in the program, and use the so-called wall-function concept. In this concept, the flux of a variable ϕ at a wall boundary, is expressed as:

$$\dot{\phi}_{\text{wall}}'' = \Gamma_{\phi, \text{wall}} \frac{\phi_{\text{near wall}} - \phi_{\text{wall}}}{\delta_{\text{wall}}} \quad (1.6-1)$$

where δ_{wall} denotes the normal distance from the wall to the near-wall point. Values of $\Gamma_{\phi,wall}$ are obtained from the presumption that in the region adjacent to wall boundaries, the dependent variables obey, for turbulent flow, a modified form of the semi-logarithmic law-of-the-wall. The formulae used to calculate $\Gamma_{\phi,wall}$ are provided in Table (1.6-1).

ϕ	$\Gamma_{\phi,wall}$
Velocity components normal to the wall	0
Velocity components parallel to the wall	$y^+ > 11.5 : \frac{\mu y^+}{\frac{1}{K} \ln [Ey^+]}$ $\leq 11.5 : \mu$
k	0
ϵ	--
All other ϕ 's	$y^+ > 11.5 : \frac{\mu}{\sigma_{eff,\phi}} \frac{y^+}{\left\{ \frac{1}{K} \ln [Ey^+] + P_\phi \right\}}$ $\leq 11.5 : \frac{\mu}{\sigma}$

Table (1.6-1)

The definition of y^+ in the table, is a generalization due to Spalding [5] of the conventional form, in that:

$$y^+ = \frac{\rho C_D^{1/4} k^{1/2} \delta}{\mu} \quad (1.6-2)$$

where δ denotes the distance from the wall, at a location with which the values of ρ and k are associated. The constants K and E in Table 1.2-2 are obtained from the conventional form of the law-of-the-wall:

$$u^+ = \frac{1}{K} \ln [E y^+] \quad (1.6-3)$$

and are given values of 0.42 and 9.0 respectively.

The boundary conditions for k and ϵ are provided as follows: the diffusion of kinetic energy k , to the wall is known to be negligible and is set to zero and a balance equation for k , regular in other respects is solved for control volumes adjacent to wall boundaries. The diffusion of dissipation rate ϵ to such boundaries is more difficult to express. Instead of attempting to calculate $\Gamma_{\epsilon, \text{wall}}$, use is made of the knowledge that the length scale l varies linearly with distance from the wall, in the neighborhood of the wall. The dissipation rate is then calculated from this length scale from:

$$\epsilon_{\text{near wall}} = C_D^{3/4} \frac{k^{3/2}}{K\delta} \quad (1.6-4)$$

The practice adopted is to fix $\epsilon_{\text{near wall}}$ to the above value, without disturbing the general calculation procedure, in the following manner:

$$\begin{aligned} S_U^\epsilon &= L \epsilon_{\text{near wall}} & (a) \\ S_P^\epsilon &= -L & (b) \end{aligned} \quad (1.6-5)$$

where L is a large number, say 10^{30} .

The expression for $\Gamma_{\phi,wall}$ for a general dependent variable ϕ , is based on the expression indicated in Table (1.6-1), the value of P_{ϕ} being calculated from:

$$P_{\phi} = 9.24 \left[\frac{\sigma_{\phi}}{\sigma_{eff,\phi}} - 1 \right] \left[\frac{\sigma_{\phi}}{\sigma_{eff,\phi}} \right]^{-1/4} \quad (1.6-6)$$

where σ_{ϕ} and $\sigma_{t,\phi}$ denote the laminar and turbulent values of Prandtl/Schmidt number appropriate to the transport of ϕ .

1.7 The treatment of compressibility

The special compressible-flow features of the computational procedure in HISS are as follows:

1.7-1 The calculation and use of density

Two distinct densities are computed and used at each step. The downstream density (ρ_P) is used only in computing the mass flux in the z-direction at the downstream face of the cell; the upstream density ($\rho_{P,U}$) is used for calculating lateral mass fluxes, and the upstream axial mass flux. The two densities are calculated as follows:

$$\rho_P = \frac{p_P W_{P,U}}{R T_{P,U}} \quad (1.7-1)$$

$$\rho_{P,U} = \frac{p_{P,U} W_{P,UU}}{R T_{P,UU}} \quad (1.7-2)$$

where W_P is the local mixture molecular weight, R is the universal gas constant, and subscript 'UU' refers to the plane two steps upstream of the plane in question.

1.7-2 The momentum equation in the z-direction

The source term employed in the w equation depends on whether the local flow is subsonic or supersonic. When the flow is subsonic it is necessary^{*}, in order to render the equations parabolic, to write the source term as a mean pressure gradient, i.e.,

$$S_w \equiv \frac{d\bar{p}}{dz} = \frac{\bar{p} - \bar{p}_U}{\delta z} \quad (1.7-3)$$

where \bar{p} denotes the mean pressure which is determined for a confined flow from the requirements of overall continuity, as described in reference [5]; for an unconfined flow, \bar{p} is simply the free-stream pressure.

* The need for this practice is discussed in reference [5].

For supersonic flow, in contrast, it is possible, without destroying the parabolic nature of the equations, to employ the local pressure to calculate the pressure gradient, i.e.,

$$S_w = \frac{\partial p}{\partial z} = \frac{p_p - p_{p,U}}{\delta z} \quad (1.7-4)$$

This practice, it should be observed, allows full account to be taken of pressure waves in supersonic flow.

1.7-3 The pressure-correction equation

The incompressible-flow form of the pressure-correction equation given in reference [5]* must, in order to handle compressible flow, be modified as described below.

Account must now be taken of the effect of a pressure change at P on the mass flux at the downstream face of the cell. For supersonic flow the mass-flux change $(\rho w)_p'$ is related to the pressure correction p_p' by:

$$(\rho w)_p' = [\rho_p^* D_p^w + \left(\frac{d\rho}{dp}\right)_p w_p^*] \cdot p_p' \quad (1.7-5)$$

where, ρ_p^* and w_p^* are computed from the guessed pressure p_p^* , $(d\rho/dp)_p$ is, from equation (1.7-1):

$$\left(\frac{d\rho}{dp}\right)_p = \frac{w_{p,U}}{R T_{p,U}} \quad (1.7-6)$$

and

$$D_p^w = \frac{w_p'}{p_p'} \quad (1.7-7)$$

and is deduced from the finite-difference form of the momentum equations, in the manner described in reference [5].

* Note that in reference [5] the forward-marching direction is the x direction, whereas in HISS it is the z direction.

For subsonic flow, equation (1.7-5) must be modified to account for the fact that w_p no longer depends on p_p ; the modified expression is:

$$(\rho w)'_p = \left(\frac{d\rho}{dp} \right)_p \cdot w_p^* \cdot p_p' \quad (1.7-8)$$

The resulting equation for p' is of the form given in reference [5] with the coefficients modified to account for the above-described influences of p_p' on $(\rho w)'_p$.

2. GENERAL FEATURES OF HISS

2.0 Introduction

In this chapter an overview of HISS is given with a description of the program flow and control, and definitions of important variables.

2.1 General structure

The general structure of the HISS computer program is shown in Figure (2.1-1). The divided, vertical box on the left is the main program, HISS, which has the chief function of controlling the calling sequence of the subprograms. The starting point for HISS is at the top of this box. Points where call of subprograms are made in HISS are denoted by horizontal lines. Arrows indicate the "flow" of the computer program to and from the subprograms which are shown in boxes. The major calculations and logical decisions made by HISS are indicated in the spaces between the horizontal lines marking calling points in HISS.

The subprograms are contained in subroutines which are not individually called. These subroutines can be classified in three categories: problem dependent, physical property dependent and invariant. BLOCK DATA and ALLMOD are the problem dependent subroutines while AUX is for physical property specification. SOLVE, STRIDA, STRIDB and PRINT are the invariant portions of the program.

The remaining part of this chapter gives a general overview of the computer program while the next chapter details the operation of each subroutine.

2.2 Fortran equivalents of main variables

A few of the FORTRAN names used in HISS which will be required in the following sections, are introduced here. The dependent variables ϕ are stored in an array F, which it is convenient to consider as a three-dimensional array F (I,J,NV). Here I and J denote the location (respectively along the x and y directions) and NV identifies a particular variable. The three velocity components and the pressure-correction are included in the F array; however, for ease in understanding, separate arrays U,V,W and PP are also used and made equivalent to parts of F as

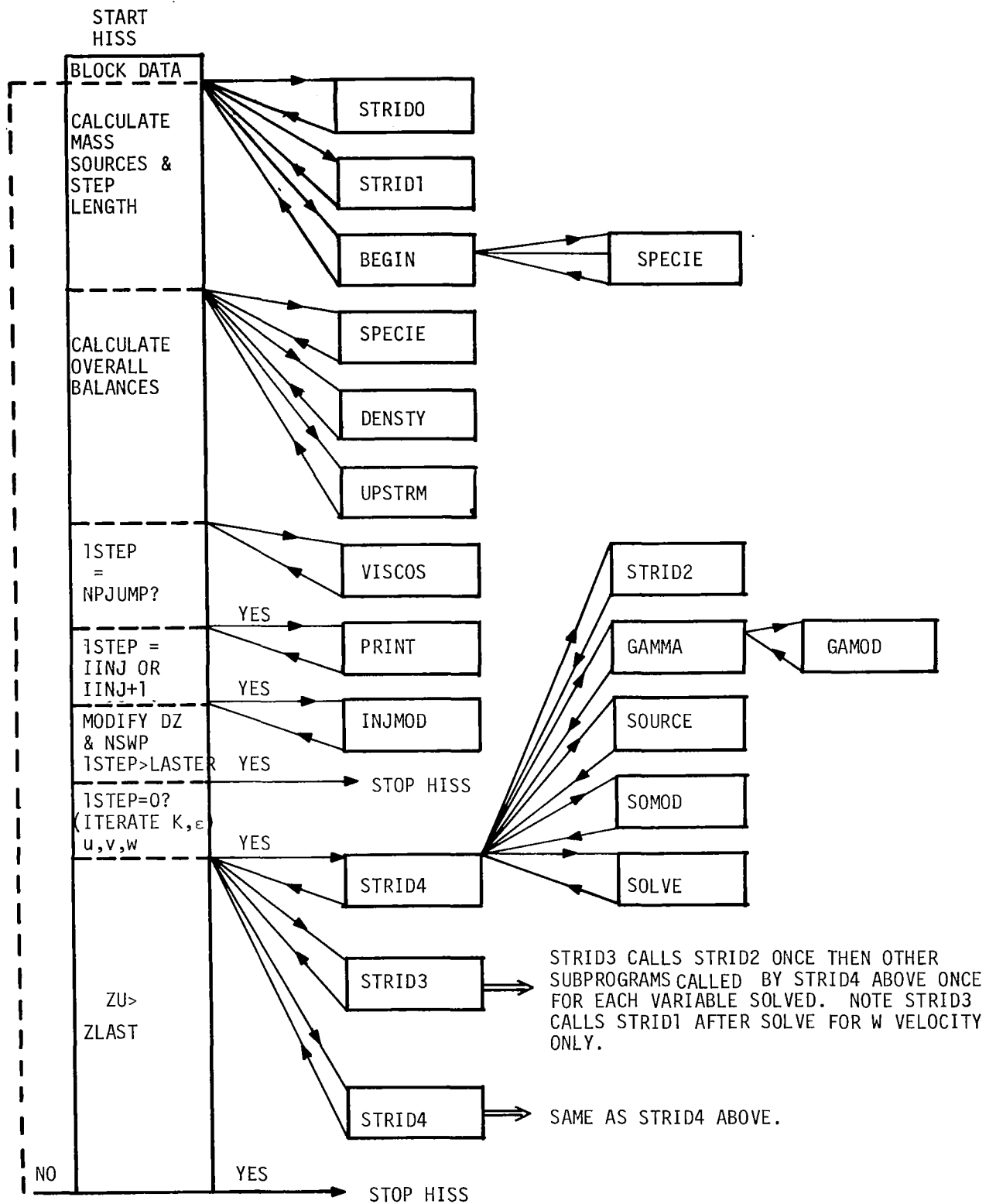


Figure 2.1-1. General Structure of HISS Computer Program

follows:

$$\begin{aligned}U(I,J) &\equiv F(I,J,NVU) \\V(I,J) &\equiv F(I,J,NVV) \\W(I,J) &\equiv F(I,J,NVW) \\PP(I,J) &\equiv F(I,J,NPP)\end{aligned}\tag{2.2-1}$$

The identifiers NVU, NVV, NVW and NPP, also used to identify U,V,W and PP elsewhere in the program, are assigned values 2,3,4 and 1. The largest values of I,J and NV for which storage is provided in the program are denoted by IMAX, JMAX and NNV respectively and assigned values 12, 34 and 9.

Although two- and three-dimensional arrays have been mentioned above, the computer program formally uses one-dimensional arrays, whose subscripts are calculated, each time they are required. Thus, $F(I,J,NV)$ is referred to as $F(IJNV)$, where:

$$IJNV = I + JM(J) + NFM(NV)\tag{2.2-2}$$

the arrays JM and NFM being calculated once-and-for-all from:

$$\begin{aligned}JM(J) &= (J - 1) * IMAX \\NFM(NV) &= (NV - 1) * IMAX * JMAX\end{aligned}\tag{2.2-3}$$

Also $W(I,J)$ is referred to as $W(IJ)$ where:

$$IJ = I + JM(J)\tag{2.2-4}$$

The four neighboring points of the location IJ, corresponding to the points of the compass are referred to as IJ_N , IJ_S , IJ_E and IJ_W . These are calculated as:

$$\begin{aligned}
IJN &= IJ + IMAX \\
IJS &= IJ - IMAX \\
IJE &= IJ + 1 \\
IJW &= IJ - 1
\end{aligned}
\tag{2.2-5}$$

It is easy to see that points further removed become:

$$\begin{aligned}
IJNE &= IJN + 1 \\
IJSW &= IJS - 1 \quad \text{etc.}
\end{aligned}
\tag{2.2-6}$$

For a given problem, all members of the F array for which provision is available, may not be required to be solved for. Furthermore, some of these variables may be obtained from algebraic equations and not from the solutions to the partial differential equation. To provide for these alternatives, use is made of an array ISOLVE(NV). For ISOLVE(NV) equal to zero, the differential equation is not solved; solution is obtained for values of ISOLVE(NV) greater than zero. It is left to the user, to make further use of this facility.

Other arrays directly related to members of the F array are: IPRINT(NV), FU(IJ,NV), TITLE(K,NV), FLUXN(I,NV), FLUXS(I,NV). Values of F(IJ,NV) are printed out if IPRINT(NV) is equal to 1; otherwise, a printout is not obtained. FU(IJ,NV) stores the upstream value of F(IJ,NV) during the iteration cycle at any given integration station. FLUXN(I,NV), stores the fluxes of the variable NV, on the North boundary and FLUXS(I,NV) is for the South boundary. TITLE (K,NV) with the integer K taking values 1 to 9, stores a 36 character alphanumeric title of the corresponding variable NV. This is used to identify the values of the variables in the print-out.

The quantities k, ϵ , h, f, and T form the remaining variables of the F family. They are identified by the indices NVK, NVD, NVH, NVF, and NVT respectively and occupy NV locations 5,6,7,8 and 9 in the array F(IJ,NV). No equation is solved for T; however, it is convenient to store it at F(IJ, 9). Quantities p, ρ and Γ are stored as P(IJ), RHO(IJ) and GAM(IJ). They are not members of the F array, but are included along with F in a COMMON

statement, and immediately following it. They can therefore be referred to as the $(NNV + 1)^{th}$, $(NNV + 2)^{th}$ and $(NNV + 3)^{th}$ members of the F array, as indeed they are in subroutine PRINT. The integers NVP, NRO and NMU are used to identify them.

Although, in general, the values of Γ are different for each dependent variable, storage provision for only one set of Γ 's is retained. Hence, at a given stage in the program, the GAM array contains the values of Γ , appropriate to the dependent variable under consideration. Similarly, provision is made for the retention of one set of coefficients of the finite-difference equation at a given stage. Thus, AXP(IJ), AXM(IJ), AYP(IJ), AYM(IJ) and AZ(IJ) respectively represent the coefficients A'_E , A'_W , A'_N , A'_S and L_U in equation (1.4-5). Similarly, SU(IJ) and SP(IJ) represent S_U and S_P respectively in equation (1.4-3). The quantities like $D_{P,U}$ in reference [5] are stored as DU(IJ), there being similar arrays, DV(IJ) and DW(IJ), for the corresponding quantities associated with the v- and w- momentum equations.

KBCN and KBCS denote the type of North and South boundary respectively as follows: 1 indicates symmetry, 2 indicates solid wall, and 3 indicates a free boundary.

2.3 Program control

Program control, including start, internal monitoring and stop functions, is achieved through program DAVE.

Using the information supplied through BLOCK DATA, the first part of DAVE calculates and assembles all the information about the grid system through calls to STRID0 and STRID1. Following this, in the same part, a call to BEGIN, supplies the initial conditions for all the dependent variables.

The second part begins with the statement: 60 CONTINUE. Following this, mass sources, step length and the location of the station for the new calculation, are determined. This is followed by calls to SPECIE, DENSTY and UPSTRM. SPECIE calculates the chemical specie composition from element compositions, temperature and pressure. DENSTY is a member of the physical modelling subroutine AUX, wherein the fluid density ρ , is calculated. UPSTRM stores the upstream variables required by the

computation in the array FU. After calculating the overall balance of the major F arrays a call is made to VISCOS which calculates τ . If ISTEP equals NPJUMP profiles of variables specified by IPRINT(NV) = 1 will be printed out. Otherwise, only overall balance information and station location will be printed out.

The next section is for the calculation of the velocity and pressure fields. First, a check is made to see if injection occurs. If this test is positive, a call is made to INJMOD which provides the appropriate boundary conditions through source terms. Next a check is made to determine whether the station for calculation is immediately downstream of injection. If this test is positive the number of sweeps on the pressure correction equation and the step length are modified to increase accuracy and stability of the program. The calculation is stopped at this point if ISTEP > LASTEP. Next a check is made to determine if ISTEP = 0 which if positive, results in iteration on the hydrodynamic and turbulence equation to improve the starting profile.

After this series of tests, a call is made to STRID3 which yields the velocity and pressure fields. A call to STRID4 performs similar calculations for all other dependent variables. If ZU < ZLAST, control is returned to a point in DAVE just after the CALL BEGIN statement and the process repeated for the next station.

2.4 Detailed list of program variables

All variables used in common statements are defined in Appendix B. Variables which appear locally are defined by their use in the computer program and are not defined in this report.

3. INVARIANT PORTIONS OF HISS

3.0 Introduction

Many of the calculations do not need changing for different boundary conditions, etc. In this chapter the function of each invariant portion of HISS is given. Again important variables are defined.

3.1 Calculation of grid quantities

The two sets of grid quantities specified by the user in BLOCK DATA are LCV, MCV and ZETA(I), AGEOM. The former represent the number of ϕ -control volume faces in the x and y directions and the latter the non-dimensional coordinate distributions of the ϕ -locations in the x direction.

Given the above information, STRIDØ, the first member subroutine of STRIDA, computes the maximum number of grid nodes in the I and J directions. This is done in the following sequence:

$$\begin{aligned} L &= LCV + 1 \\ M &= MCV + 1 \\ LP1 &= L + 1 \\ MP1 &= M + 1 \end{aligned} \tag{3.1-1}$$

It is emphasized here that users must ensure that LP1 and MP1 are always less than or equal to IMAX and JMAX respectively. The latter represent the maximum dimensions of all variables in the respective directions and are given values accordingly in BLOCK DATA. STRIDØ is concluded with the specification of the integer arrays JM and NFM in accordance with equation (2.2-3).

The second member of STRIDA is STRID1. STRID1 is called once from HISS. It is in STRID1 that the physical coordinates x and y are computed from the values of AGEOM and ZETA, as follows:

$$\begin{aligned} X(I) &= ZETA(I) * BXE \\ Y(J) &= Y(J - 1) + AGEOM ** (J - 2) * DELY \end{aligned} \quad (3.1-2)$$

where $DELY = BYN * (1.0 - AGEOM) / (1.0 - AGEOM ** M)$. Here BXE and BYN represent the width and height of the calculation domain respectively; as such, they are to be specified by the user in `BLOCK DATA`. The above specification of $Y(J)$ makes use of a geometric series for specifying successive intervals between $Y(J)$ and $Y(J - 1)$. Larger values of $AGEOM$ result in the grid being "crowded" closer to the $Y = 0$ surface.

Figure (3.1-1) now shows the grid in plane for a Cartesian coordinate system and illustrates the nomenclature described below.

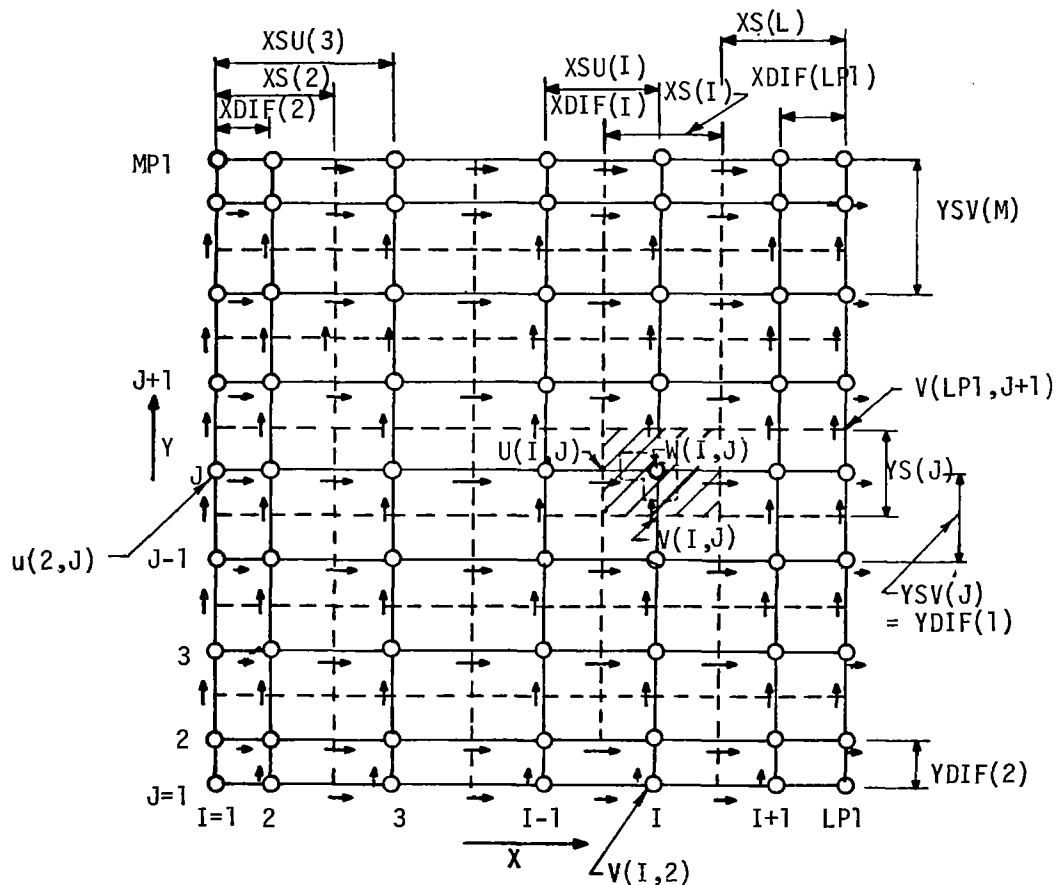


Fig. (3.1-1) Grid showing numbering, main control volumes and FORTRAN definition of grid quantities. (Cartesian coordinates)

The dashed lines in Figure (3.1-1) join the control-volume faces normal to the x and y directions. These are the control volumes for all dependent variables except the U and V velocity components. The control-volume faces pass mid-way between the grid nodes except near the boundaries where they pass through the boundary grid nodes. Thus, the control-volume faces always pass through points where the velocity component normal to the faces are stored. A normal velocity component at a control-volume face is presumed to prevail over that whole face.

The control volumes for each of the velocity components U and V are displaced along the directions of these velocities. The control-volume faces normal to each of these directions pass through grid nodes on either side of the velocity component in question. Figure (3.1-2) illustrates this point. The geometric quantities associated with this grid system are defined in Table 3.1-1.

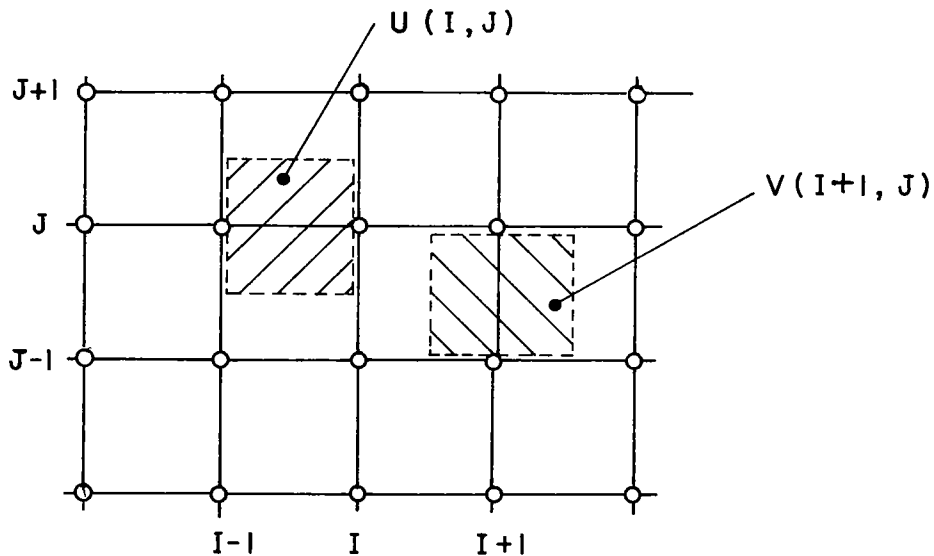


Figure 3.1-2 U- and V- Velocity Control Volumes

TABLE 3.1-1

NO.	GRID QUANTITY	MEANING
1	X(I)	Physical coordinate in the x-direction.
2	XDIF(I)	The difference between X(I) and X(I-1); used as the distances δ in calculating x-direction diffusion flux of ϕ : $\Gamma_{\phi} \Delta\phi / \delta$.
3	XS(I)	The x-direction width of a main control volume.
4	XSU(I)	The x-direction width of a U-velocity control volume.
5	Y(J)	Physical coordinate in the y-direction.
6	YDIF(J)	The difference between Y(J) and Y(J-1); used as the distances δ in calculating y-direction diffusion flux of ϕ .
7	YS(J)	The y-direction width of a V-velocity control volume.
8	YSV(J)	The y-direction width of a V-velocity control volume.

Because the faces of the main control volumes are stipulated to pass midway between the grid nodes, interpolation factors for the calculation of variables on these faces are equal to 0.5, except near boundaries where they are either 0 or 1. For the control volumes appropriate to U- and V- velocity components, however, the interpolation factors can differ from 0.5, if the spacing between grid nodes is chosen to be non-uniform. For this reason, interpolation factors are calculated in STRID1 and stored as FXP(I), FXM(I), FYP(J) and FYM(J). The subscript refers to a grid node. The value of U for example at a grid node (I,J) is given by:

$$FXP(I) * U(I + 1,J) + FXM(I) * U(I,J) \quad (3.1-3)$$

it is obvious from the above that FXM(I) is simply 1.0 - FXP(I).

Calculation of the quantities tabulated above completes the tasks performed by STRID1. STRID1 is called once from DAVE to calculate the initial grid quantities. Also, STRID1 is called from STRID3, after the W- velocity equation is solved and corrected for.

3.2 Assembly of coefficients

STRID2

The STRID2 portion of STRIDA is used to calculate and store the convective mass velocities (i.e. ρu , ρv and ρw in equation 1.2-1, crossing the control volume faces along the x and y directions). The arrays GX and GY are used, respectively, to store these values.

STRID2 is called, for each integration plane, once at the beginning of STRID3. Finally, STRID2 is called from STRID4, after the U- and V- velocities have been corrected.

STRID3

As referred to briefly above, STRID3 and STRID4 are the component subroutine of STRIDB which can be regarded as the main machinery of the HISS program. It is in STRID3, that the finite-difference equations appropriate to U,V,W and p' are assembled, in that order. After the appropriate equations are assembled, a call is made to SOMOD (a member

subroutine of ALLMOD) to determine whether any coefficients of the equations require modification. Once this is achieved, a call to SOLVE permits solutions of the finite-difference equations to be obtained. Once this preparation is completed, the coefficients of the pressure-correction equation set are assembled and the equations solved. STRID3 is then concluded with a section in which U's, V's and p's are corrected.

STRID4

The assembly of and solutions to the finite-difference equations of all other dependent variables are performed in STRID4. The primary reason for keeping the functions of STRID3 and STRID4 apart is to permit iterations to be performed separately on each of these subprograms. The iterations themselves are initiated by the controlling subprogram MAIN. This iteration is used in HISS to obtain better distribution of K and ϵ for the initial step.

3.3 Solution procedure for algebraic finite-difference equations

SOLVE

The function of the subprogram SOLVE is to arrange for the solutions to the finite-difference equations for each dependent variable NV, to be obtained. The solution procedure used is the application of a pair of Standard Tri-Diagonal Matrix (TDMA) traverses, one in each of the x and y directions.

SOLVE has three major subdivisions. The first ends with the statement: 10 CONTINUE. It is in this part that the finite-difference coefficients are assembled in readiness for the subsequent operations. Fully-implicit practices are employed during the coefficient-assembly process.

The second part of SOLVE is concerned with TDMA traverses in the x direction and ends with statement: 21 CONTINUE.

The third and final part of SOLVE starts with this statement and concerns the TDMA traverses in the y direction.

A call to SOLVE is made from STRID3 and STRID4, once for each dependent variable NV. This call achieves TDMA traverses in both the x and y directions; however, which traverse is made first depends upon the value of the index IXY. The first traverse direction will be x if IXY = 1, and y

if IXY=2. IXY is set alternately to 1 or 2 by the statement: IXY=3-IXY which concludes both STRID3 and STRID4. The order of solution for problems for which HISS is applicable is not important.

Along each traverse direction, the direction of sweep, i.e. whether from the first grid node to the last or vice versa, depends upon the value of an index, ISWP in the x direction and JSWP in the y direction. Each of these indices takes on a value 1 or 2 by statements which follow the end of parts 2 and 3 of SOLVE. For example, the statement following: 21 CONTINUE, reads: JSWP = 3 - JSWP. A value 1 implies that the sweep direction is from first to last grid node and 2 implies vice versa.

On occasion, it may be required to perform more than one pair of TDMA traverses in a x-y plane, for any given dependent variable. The number of pairs of TDMA traverses is set by values assigned to an index array NSWP(NV). The program is set up with NSWP values equal to three except for the pressure-correction equation for which NSWP(NPP) = 6.

3.4 Printout of field values of dependent variables

PRINT(ISKIP, JSKIP)

It is frequently required to print out the contents of the F array. This task is performed by subroutine PRINT.

PRINT(ISKIP, JSKIP) provides for the printout of F(I,J,NV) where NV can attain a maximum value of NFPMAX, which is set as:

$$NFPMAX = NNV + 3 \quad (3.4-1)$$

The three extra values representing NVP, NRO and NMU, i.e. pressure, density and effective viscosity respectively. The decision as to whether a particular variable NV is printout or not, depends upon whether the corresponding IPRINT(NV) is equal to unity or not.

The printout of each dependent variable NV is given a heading stored in TITLE(...,NV). The formal parameters ISKIP and JSKIP permit the selective skipping of columns (I) and rows (J), when it is not required, for any reason, to printout the complete array of values of each variable.

4. PHYSICAL MODELLING

4.0 Introduction

This chapter describes the portion of HISS which calculates the physical properties required in the solution procedure.

4.1 AUX

The general policy is to confine all tasks associated with physical modelling to subprogram AUX. Thus, the calculation of density ρ , effective diffusion coefficient Γ and sources and sinks s of the dependent variables are performed in separate member subroutines of AUX. There are five such subprograms in AUX, namely, DENSTY, VISCOS, GAMMA, SOURCE, and SPECIE.

DENSTY

This subroutine calculates densities $\rho_{p,U}[\text{RHO}(I,J)]$ and $\rho_p^*[\text{RHOD}(I,J)]$ in accordance with the discussion of section 1.7.

VISCOS

The function of VISCOS is to calculate the laminar and turbulent viscosity. In its present form, the major function is to store the turbulent viscosities in the array AMUT(I,J).

VISCOS also performs the function of calculating for the N and S boundaries, the effective boundary diffusion based upon the semi-logarithmic law-of-the-wall. These diffusion coefficients are stored respectively in the arrays GAMN(I) and GAMS(I).

GAMMA

GAMMA is used to set values to the array GAM(I,J). GAM(IJ) is calculated from the formula appropriate to the turbulence model [4]. A call to GAMOD is then made in order to permit any modifications to be made to the GAM array.

SOURCE

Subroutine SOURCE is used to fill the arrays SU(I,J) and SP(I,J), there being a separate section for so doing for each dependent variable. The terms that fill these arrays are finite-difference equivalents to

the source/sink terms that appear in Tables 1.2-1.

SPECIE

Subroutine SPECIE is used to calculate the specie mass fraction from knowledge of the element mass fractions, pressure and temperature. Appendix A gives a full development of the technique employed.

5. PROBLEM DEPENDENT SECTIONS

5.0 Introduction

This chapter completes the detailed description of the functions of the various portions of HISS by discussing the subroutines which must be changed in order to specify a particular problem.

5.1 General policy

As mentioned briefly earlier, the main machinery of the numerical calculation procedure is devoid of any problem-specification information. As a general policy, such information is provided through subroutines DATA and ALLMOD.

5.2 BLOCK DATA

BLOCK DATA serves to provide values to fluid properties, grid distributions, program control parameters and other information specific to each new problem, via DATA statements. The use of BLOCK DATA permits the program to be run with compilers common to both CDC and IBM machines.

5.3 ALLMOD

Subroutine ALLMOD is composed of five member subprograms BEGIN, GAMOD, SOMOD, UPSTRM and INJMOD.

BEGIN

The primary purpose of this subroutine is to provide initial values to all the dependent variable arrays, fluid-property arrays and other auxiliary arrays. The secondary purposes include provision of 'fixed' boundary conditions on the four boundaries of the calculation domain, and calculation of some auxiliary information required in the initializing process.

GAMOD

The function of modifying values of the array GAM(I,J) can be performed in GAMOD. Often, it is necessary to change only the boundary values of GAM; for instance, the diffusion coefficients relating to the

velocity component normal to a wall boundary are set to zero at the boundary itself. The incorporation of wall functions, however, is not performed in GAMOD; this function being performed in SOMOD.

SOMOD

Any desired modifications to the finite-difference coefficients AXM(I,J), AXP(I,J) etc., and to the source terms SU(I,J) and SP(I,J), can be performed in SOMOD. There is a section in SOMOD corresponding to each dependent variable. As mentioned briefly earlier, the provision of wall-functions are made through SOMOD. This is achieved as follows: first, coefficients linking boundary grid nodes with their immediate neighbors inside the calculation domain are set to zero for each variable. Then if an index, for example KBCS for the South boundary, is set equal to unity, the appropriate wall flux is calculated and fed in through SU and SP. This calculation uses the value of GAMS(I), and the corresponding flux, FLUXS(I,NV) of the dependent variable is stored for purposes of printout. If the index is other than unity, no change is made to the coefficients. A similar indice, KBCN, is used for the North wall. Such checks and modifications are made for the variables u,v,w,k, ϵ ,h, and f.

UPSTRM

The subprogram UPSTRM makes provisions to store upstream (i.e. previous integration plane) values of major variables. These include upstream members of the F array, stored as FU (I,J,NV), and certain other variables used in the calculations. Such a storage is required primarily for situations where iterations are resorted to and for calculation of source terms.

INJMOD

This subprogram is primarily used to specify the correct flux of a given variable through the array FINJ(NV). This array is used to modify the source term in SOMOD when injection occurs.

6. RESULTS AND CONCLUSIONS

6.0 Introduction

In this chapter comparison of predictions with experiment are given. Further, sample results for two typical cases of interest in this contract are presented.

6.1 Comparison to Experimental Data

Figure 6.1-1 shows a comparison of results computed under this contract versus experimental data from NASA [7]. These results are for normal injection of hydrogen into a supersonic air stream. The conditions are defined in reference [7]. The main parameters are as follows:

Air Stagnation Temperature	=	300°K
Air Stagnation Pressure	=	1.38 MN/m ²
Air Mach Number	=	4.05
Number of Jets	=	5
Injector Diameter	=	.1 cm
Jet Stagnation Pressure	=	.28 MN/m ²
Jet Stagnation Temperature	=	295°K
Jet Mach Number	=	1

The plot is made for a vertical plane aligned with the main flow direction and located at the center of the plate width. Three profiles of hydrogen concentration are shown at 30, 60 and 90 jet diameters downstream of the jet. Inspection of the figure shows excellent comparison between experimental and analytical results. The largest deviation occurs nearest the injector and probably can be ascribed to the elliptic nature of the flow

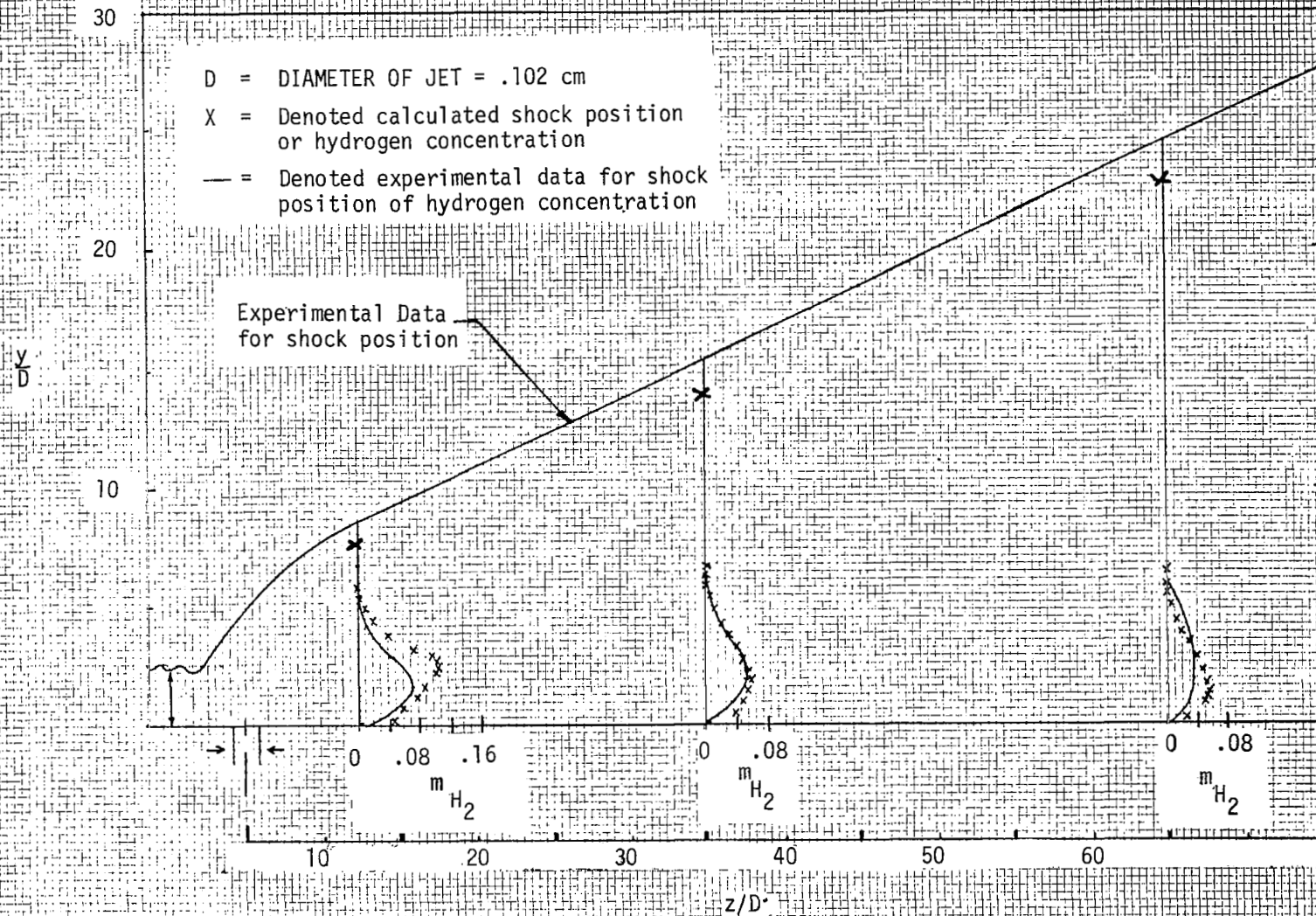


Figure 6.1-1 Comparison of Analytical Prediction with Experimental Data

in the jet region. As discussed earlier the flow was forced to be parabolic in this region. Thus, as the distance from the region increases, where the flow is parabolic, agreement between calculation and data is better.

Also shown in Figure 6.1-1 is a plot of the experimental and computed shock location. The computed shock location was taken as occurring at the peak pressure at a given station between the wall and the outer edge of the computation region. Again this comparison shows excellent correlation with experiment.

The correlation discussed above is a strong argument for the validity of the main results of this work which are described in the remaining part of this chapter. The cold flow case contains most of the physics of the cases of interest, namely supersonic compressible flow with a subsonic inner layer and strong cross stream interactions.

6.2 Presentation of Typical Results

6.2-1 Introduction

Results for ten cases were calculated for this contract by the technique described in the first five chapters. For each case profiles of 19 variables described earlier were computed for a grid of 12 grid lines transverse to the flow and 20 grid lines normal to the flow for a total of 240 points at each station in the main flow direction. Computations were made for several hundred stations. Thus, the total number of variables computed approaches nearly one-million for each case. In this section results for two typical cases will be presented. These results consist of hydrogen concentration, temperature and pressure distributions at three axial locations and at two locations transverse to the main flow direction.

6.2-2 Definition of Cases

One case for normal injection (case 1) and one case for parallel injection (case 9) are described in this chapter. The geometrical configuration of these cases are shown in Figures 6.2-1 and 6.2-2 respectively. Table 6.2 defines the flow and thermal properties.

Table 6.2 Definition of Properties

Location	Property (units)	Case 1	Case 9
Main Stream Conditions	Flow speed (m/s)	675	1585.2
	Temperature ($^{\circ}$ K)	70.6	1178.6
	Mass fraction N_2	.7676	.487
	Mass fraction O_2	.2325	.263
	Mass fraction H_2O	0.0	.25
	Pressure (N/m 2)	8720.0	179300.0
Jet Conditions	Flow speed (m/s)	1210.0	2039.4
	Temperature ($^{\circ}$ K)	250.0	150.3
	Mass fraction H_2	1.0	1.0
	Pressure N/m 2	212000.0	179300.0
	Mass flow kg/sec	.000165	.0109

6.3 Graphs of Results

All data are presented for planes normal to the wall and parallel with the main flow direction. One of these planes is located in the transverse direction directly at the hydrogen jet centerline and the other is located between jets (see Figures 6.2-1 and 6.2-2). The comparison of profiles at

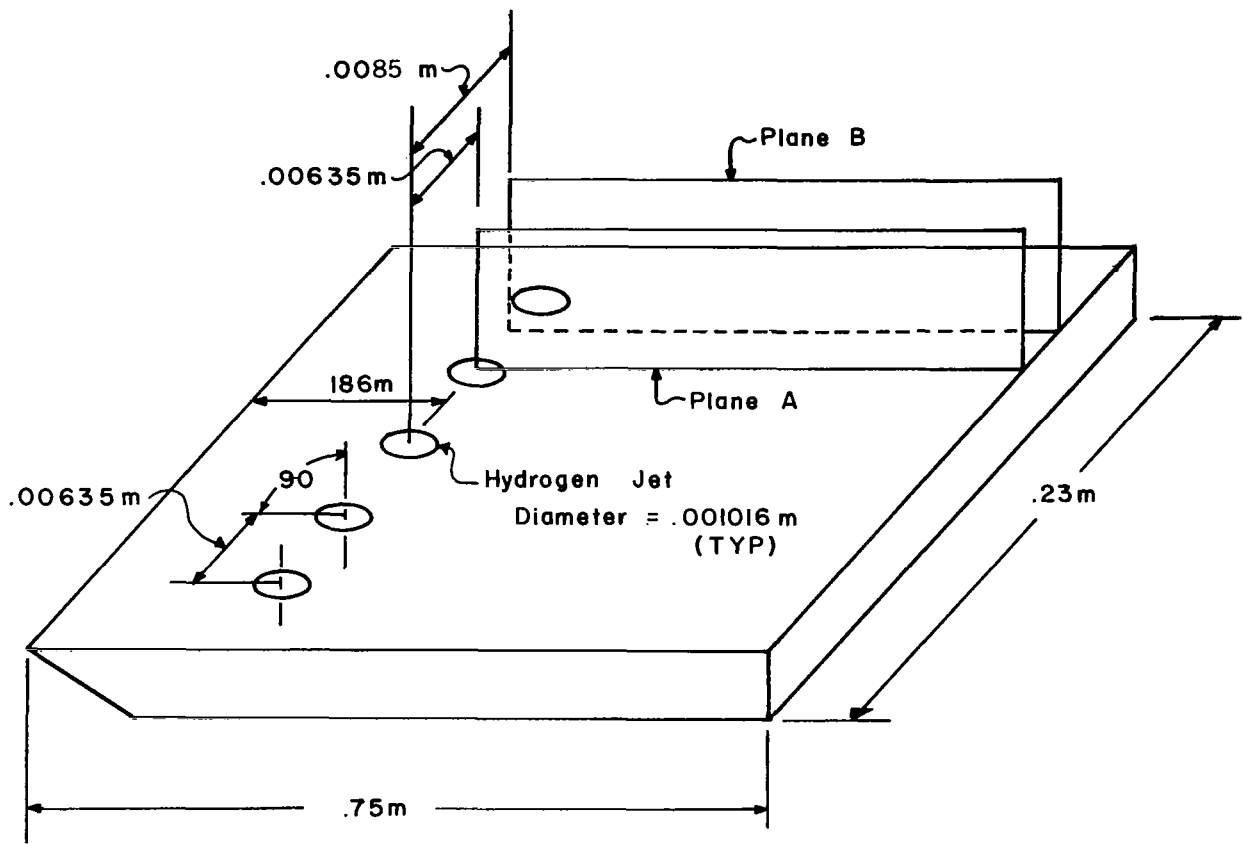


Figure 6.2-1 Definition of Geometry and Planes of Profiles for Case I

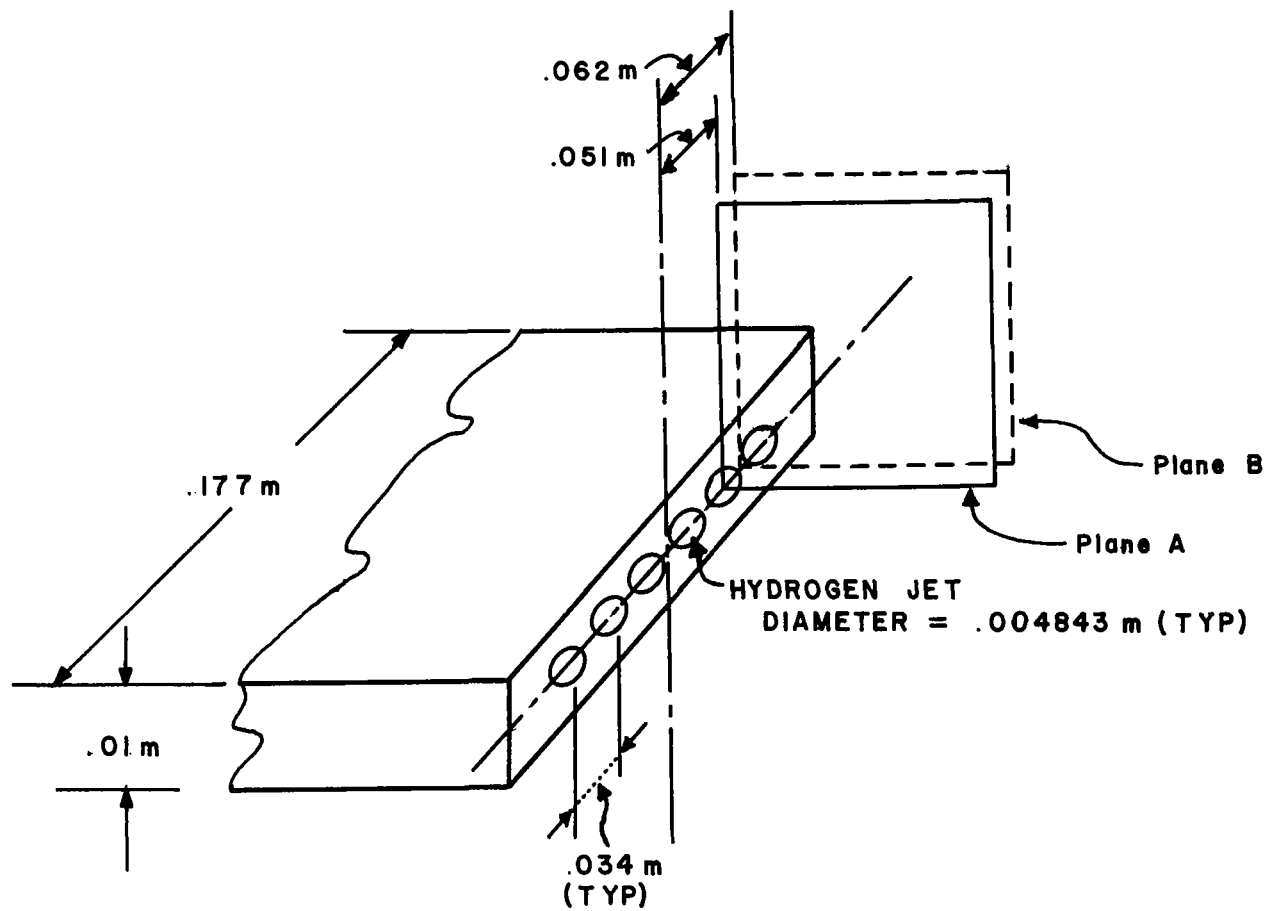


Figure 6.2-2 Definition of Geometry and Planes of Profiles for Case 9.

a given station in these two planes indicates the mixing rate in the transverse direction. Comparison of profiles in a given plane at various main flow stations indicates the rate of movement of hydrogen in a direction normal to the flow.

Figures 6.3-1 through 6.3-3 are for normal injection (case 1). Figure 6.3-1 shows the distribution of hydrogen in any form at three axial locations (.118m, .216m and .246m). The first profile is before the injection point (.196m) and therefore no hydrogen is present. At the .216m location, the hydrogen concentration levels (less than .01) indicate that substantial mixing has occurred, and the profiles indicate that mixing is primarily in the y direction. (The close spacing of the adjacent injectors limits x direction mixing.) Examination of the results at the .246m station shows continuing movement of hydrogen upward with an attendant smoothing of the profile, as would be expected.

The temperature profiles of Figure 6.3-2 indicate that after injection and combustion that little transverse thermal gradient exists. This is partly due to the fact that the flame front is at the outer layer of the hydrogen zone which tends to diffuse the temperature in the transverse direction. Also it is seen that the reaction of hydrogen moves the thermal boundary layer outward from the plate with movement in the main flow direction.

The pressure distribution for case 1 is shown in Figure 6.3-3. It exhibits the qualitative behavior one would expect. There is little transverse pressure difference due to the low velocities in that direction. A pressure spike can be seen downstream of the jet indicating a shock. The pressure below the shock is essentially uniform at a higher value than the free stream. It must be emphasized that the pressure distribution in the jet region is subject to error due to the fact that the flow

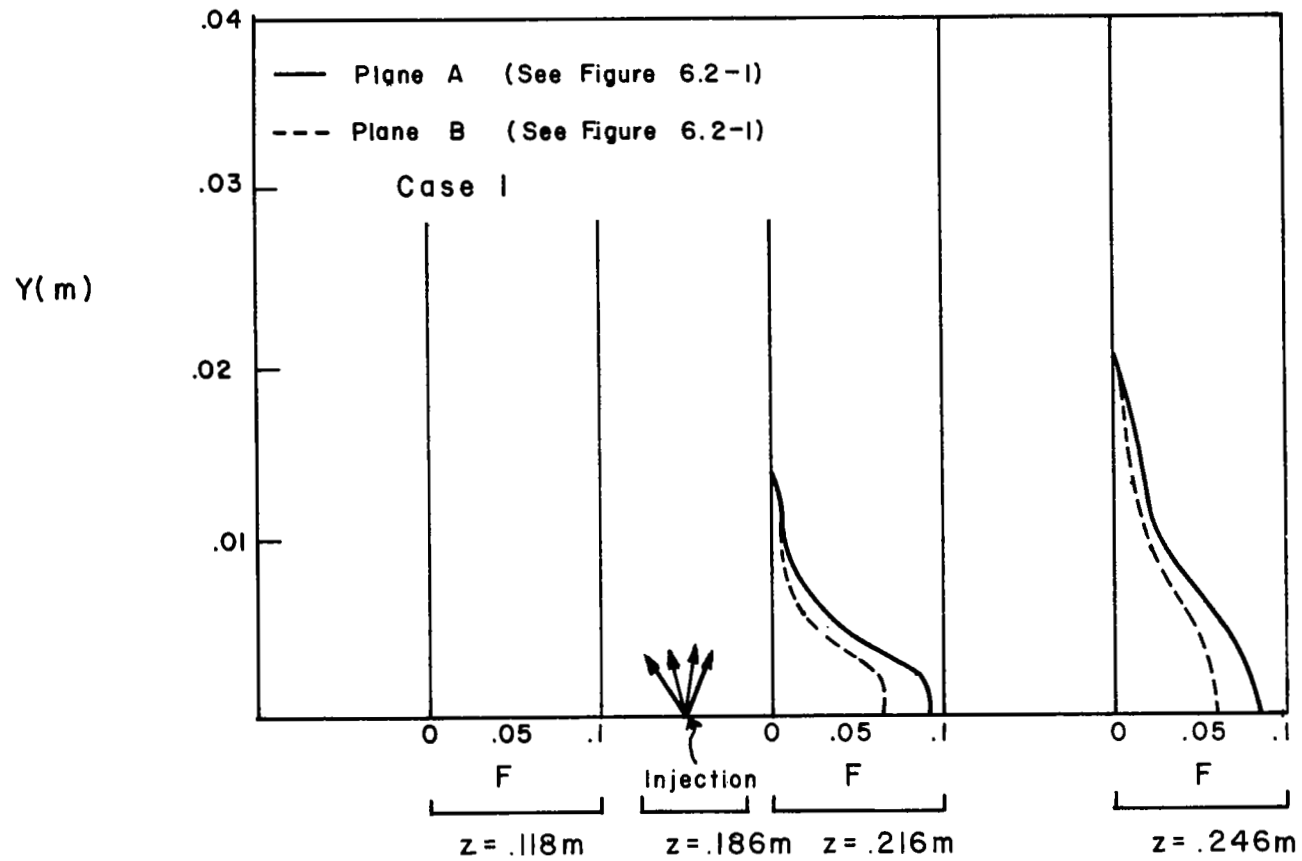


Figure 6.3-1 Distribution of Hydrogen in any form for Case I

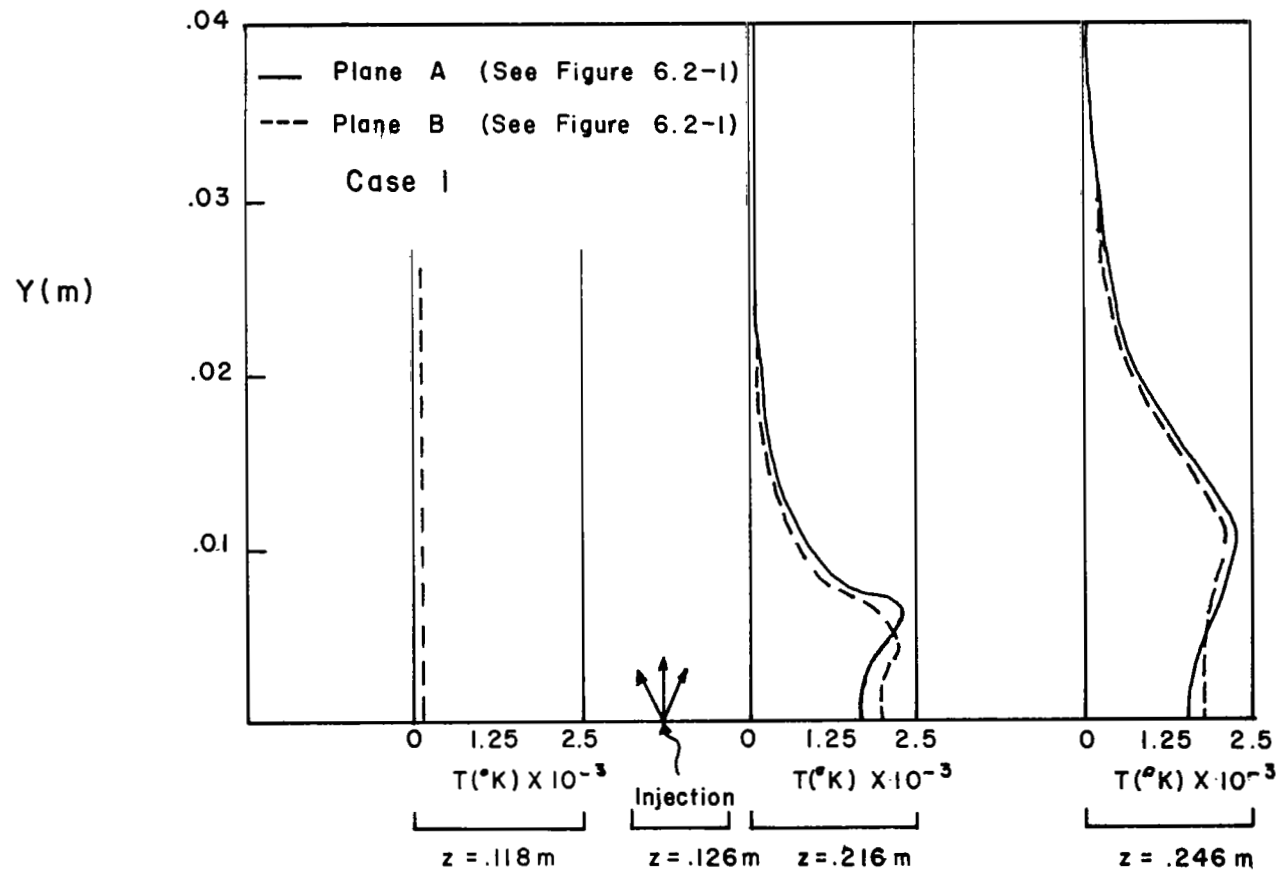


Figure 6.3-2 Temperature Distribution for Case I

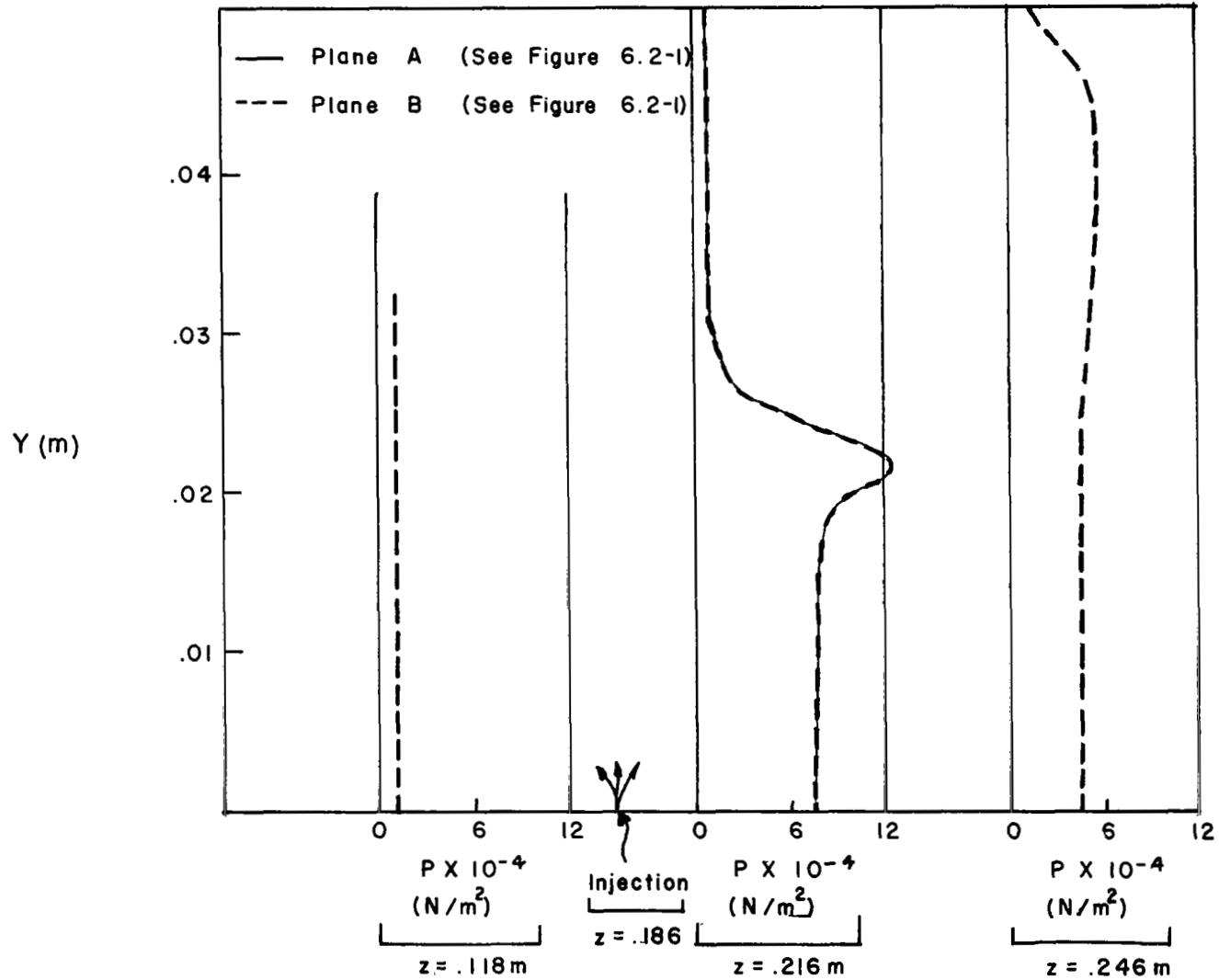


Figure 6.3-3 Pressure Distribution for Case I

was forced to be parabolic when in actuality there is some upstream effect caused by the jet.

Figures 6.3-4 through 6.3-6 are results for case 9 which is parallel injection. The diameter of the jets and jet spacing are much larger than for case 1. The profiles at injection ($Z=0$) show that there is little mixing of hydrogen between jets. However, as the flow moves forward the mixing increases such that the concentration of hydrogen between jets is roughly 50% of the hydrogen concentration in line with the jet at $Z=.36$ meter. However, these figures show that in the normal direction the movement of hydrogen upward between jets is not very effective. This is due to the low normal velocities for the parallel injection case. The temperature distribution in Figure 6.3-5 indicates a higher temperature between jets even though the hydrogen concentration is lower. This is because the combustion occurs at the fringe of the hydrogen zone. The combustion zone upper surface is indicated by the "spikes" in the temperature profile. This combustion is seen to grow with movement downstream. The pressure distribution shown in Figure 6.3-6 does not indicate any shocks. At the injection station ($Z=0$), the flow expands in the low density region. However, at downstream locations the pressure becomes uniform at approximately the free stream value.

6.4 Conclusions and Recommendations

Qualitatively the results calculated by the method developed herein appear to be correct. Further comparison with cold flow data also show excellent agreement. The computational time for these results is excellent (1 minute on a CDC 7600).

The assumption of parabolic flow in the injection region needs improvement because both data and calculations made in this work indicate that the pressure distribution is affected upstream by the jet. Recirculation, however, is probably not important. What is needed is a technique to allow

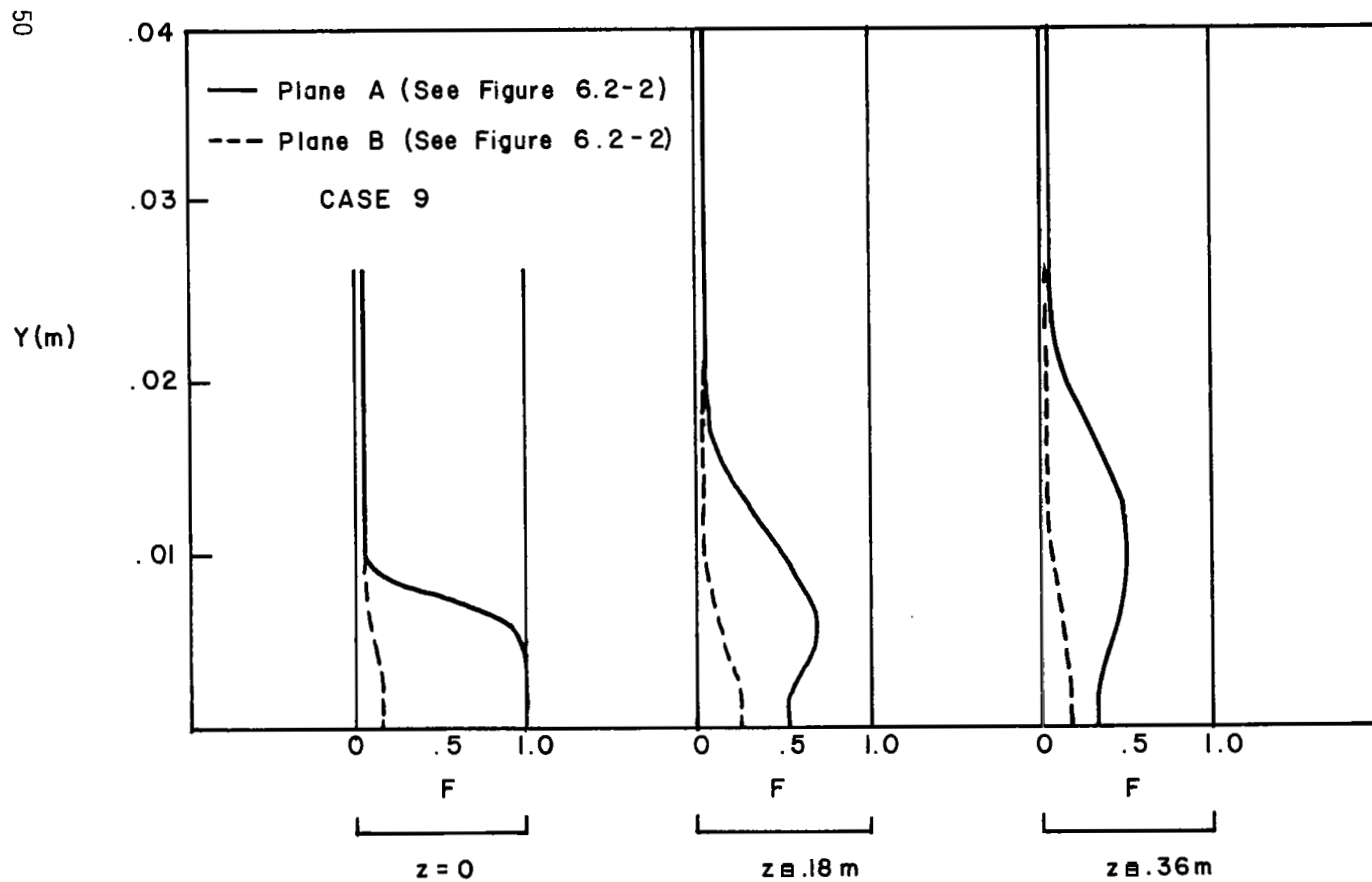


Figure 6.3-4 Concentration of Hydrogen in any form

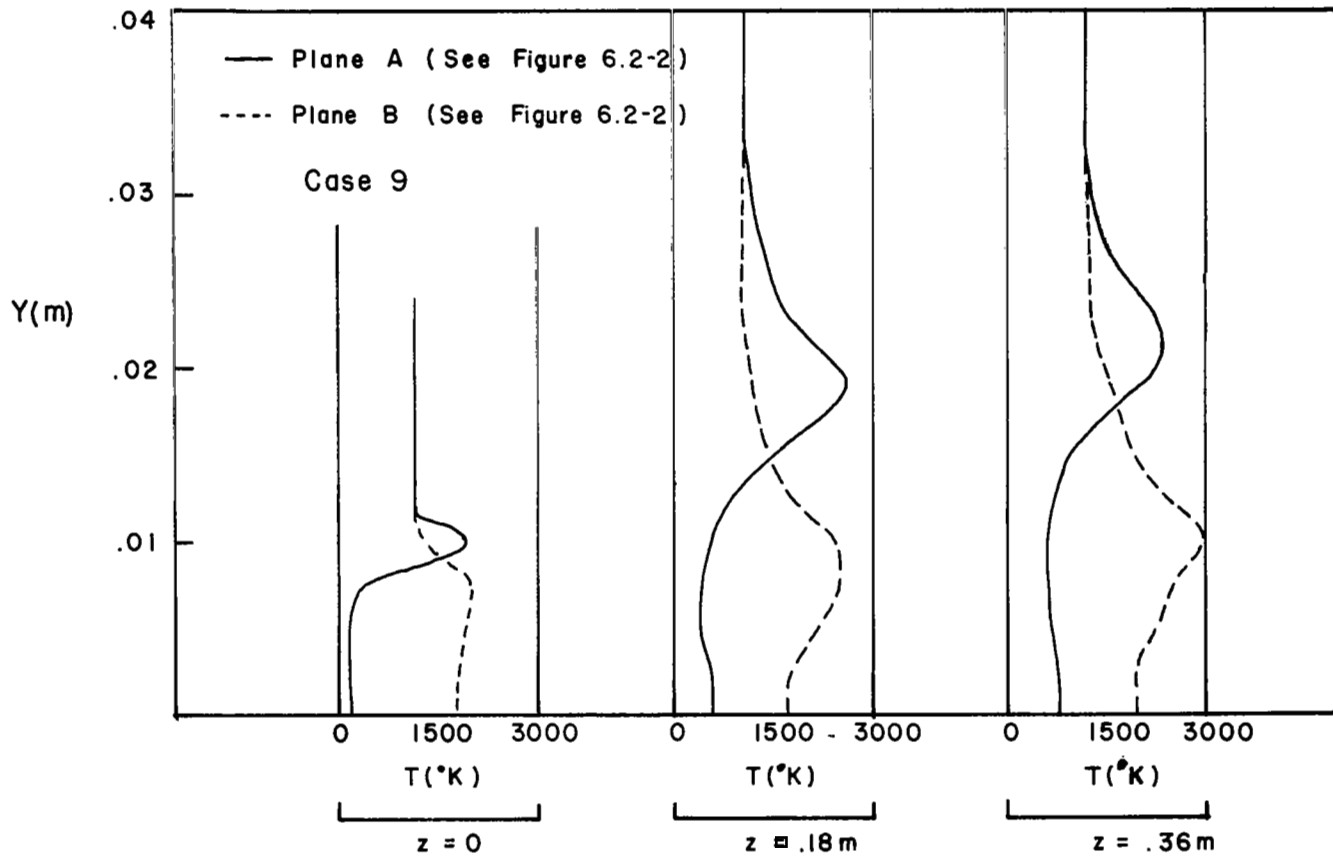


Figure 6.3-5 Temperature Distribution for Case 9

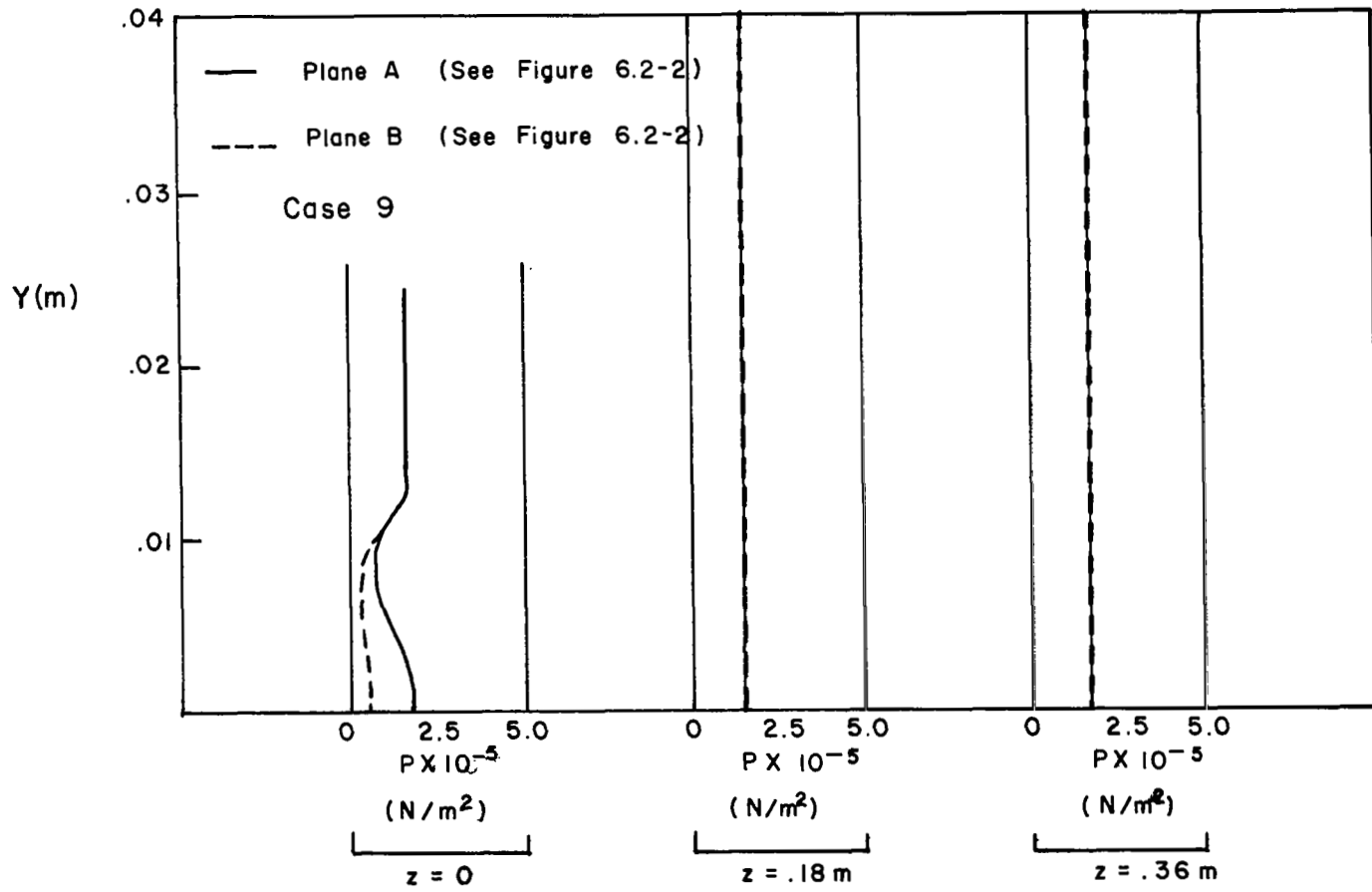


Figure 6.3-6 Pressure Distribution for Case 9

the pressure to be calculated via an elliptic procedure and the velocity by a parabolic one. Such a technique is advantageous over fully elliptic procedure because storage and computation time are much lower.

7. REFERENCES

1. Rogers, R. C., Mixing of Hydrogen Injected from Multiple Injectors Normal to a Supersonic Airstream, NASA TN D-6476, 1971.
2. Anderson, G. Y. and P. B. Gooderum, Exploratory Tests of Two Strut Fuel Injectors for Supersonic Combustion, NASA TN D-7581, 1974.
3. Rogers, R. C. and J. M. Eggers, Supersonic Combustion of Hydrogen Injected Perpendicular to A Ducted Vitiated Airstream, AIAA Paper Number 73-1322, November 1973.
4. Launder, B. E. and D. B. Spalding, Mathematical Models of Turbulence, Academic Press, London, 1972.
5. Patankar, S. V. and D. B. Spalding, A Calculation Procedure for Heat, Mass and Momentum Transfer in Three-Dimensional Parabolic Flows, International Journal of Heat and Mass Transfer, Vol. 8, No. 15, 1972, pp. 1787-1806.
6. Spalding, D. B., B. E. Launder, A. P. Morse and G. Maples, Combustion of Hydrogen-Air Jets in Local Chemical Equilibrium, NASA CR-2407, 1974.
7. Rogers, R. C., Mixing of Hydrogen Injected from Multiple Injectors Normal to a Supersonic Airstream, NASA TN D-6476, 1971.

8. NOMENCLATURE

C_D	turbulence constant (Table 1.2-2)
C_p	specific heat
C_1	turbulence constant (Table 1.2-2)
C_2	turbulence constant (Table 1.2-2)
E	law of wall constant (Table 1.2-2)
f	mass fraction hydrogen in any form
\bar{h}	stagnation chemical enthalpy $(\sum m_{f_i} h_i^o + \frac{u^2+v^2+w^2}{2} + C_p (T-T_{ref}))$
h_i^o	enthalpy of formation
k	kinetic energy of turbulence
K	constant in law of wall (Table 1.2-2)
m_{f_i}	mass fraction of specie i
p	pressure
P_ϕ	parameter defined by Equation (1.6-6)
p'	pressure correction
Pr	Prandtl Number
R	universal gas constant
S_ϕ	source term for ϕ equation
T	temperature
u, u^*	corrected and uncorrected velocity in x direction
v, v^*	corrected and uncorrected velocity in y direction
w, w^*	corrected and uncorrected velocity in z direction
M	molecular weight
x	coordinate defined in Figure 1.2-1
y	coordinate defined in Figure 1.2-1
z	coordinate defined in Figure 1.2-1

NOMENCLATURE (Continued)

Γ_ϕ	conduction transport coefficient in ϕ equation
ϵ	dissipation rate of turbulence
μ	laminar viscosity
μ_{eff}	effective viscosity (laminar + turbulent)
μ_t	turbulent viscosity
ρ	density
σ_ϕ	laminar Prandtl or Schmidt Number for ϕ
$\sigma_{t,\phi}$	turbulent Prandtl or Schmidt Number for ϕ
ϕ	general dependent variable in conservation equation

SUBSCRIPT

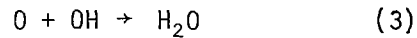
ref	reference value
-----	-----------------

APPENDIX A

A.0 Background

Reference [6] describes an equilibrium chemistry model developed and used in conjunction with a computer program to predict the properties in a hydrogen-oxygen flame. The main features of the model are described below.

Four equilibrium reactions are assumed as follows:



The six species involved in these reactions are considered to be present with nitrogen which is inert. In developing the equations to predict the equilibrium concentration of the species, two quantities are defined, namely

$$X = m_{O_2} + m_O + \frac{W_O}{W_{H_2O}} m_{H_2O} + \frac{W_O}{W_{OH}} m_{OH} \quad (5)$$

$$F = m_{H_2} + m_H + \frac{W_{H_2}}{W_{H_2O}} m_{H_2O} + \frac{W_H}{W_{OH}} m_{OH} \quad (6)$$

where X is the total fraction of oxygen in any form and F is the total fraction of hydrogen in any form. Since the molecular weight of the various oxygen species is approximately equal to that of nitrogen it is assumed that the rate of diffusion of nitrogen is equal to that of the oxygen; and, therefore, nitrogen is present at any location in a fixed ratio to the fraction of oxygen compounds. This fraction, OFAC, is assumed constant and equal to the fraction of oxygen in the air being used as the oxidizer. Thus,

$$X = (\text{OFAC})(X + m_{N_2}) \quad (7)$$

The total mass fraction must be unity which gives

$$X + m_{N_2} + F = 1 \quad (8)$$

Substituting equation (7) into equation (8) and solving for X gives

$$X = (\text{OFAC})(1 - F) \quad (9)$$

Therefore, if F is known, X can be determined by equation (9).

From thermodynamic considerations the equilibrium constant is defined for the reaction $aA + bB \rightarrow cC$ by

$$K_p = \frac{X_C^c}{X_A^a X_B^b} P^{c-a-b} \quad (10)$$

where P is in atmospheres.

For each of the four reactions in the present model $c-a-b = -1$. It is convenient to express the concentrations in terms of mass fractions. Noting that

$$m_i = \frac{W_i}{W} X_i \quad (11)$$

and substituting equation (11) into equation (10) gives

$$K'_p \equiv K_p P^W \frac{W_C^c}{W_A^a W_B^b} = \frac{m_C^c}{m_A^a m_B^b} \quad (12)$$

Thus the equilibrium equations for the reactions (1 - 4) can be written

$$K'_1 = \frac{m_{H_2}}{m_H^2} \quad (13)$$

$$K'_2 = \frac{m_{O_2}}{m_O^2} \quad (14)$$

$$K'_3 = \frac{m_{H_2O}}{m_O m_{OH}} \quad (15)$$

$$K'_4 = \frac{m_{OH}}{m_O m_H} \quad (16)$$

The condition of equilibrium is expressed by using four equilibrium constants for the four chemical reactions. Once F and X are specified, the six species (m_{H_2} , m_H , m_{O_2} , m_O , m_{OH} , m_{H_2O}) can be determined from equations (5), (6), (13), (14), (15), and (16) in which these species are unknowns. The procedure adopted in [1] was to solve a differential equation for the distribution of F and then to solve equations (5), (6), (13), (14), (15), and (16) for the concentration of individual species. In reference [1] the values of species concentration just upstream of the point being considered were used to choose the largest term in both F and X. The mass fractions of remaining species were calculated from equations (13 - 16) using the upstream temperature for specifying the equilibrium constants and the values of the upstream species mass fraction which constitute the largest terms in F and X. New values of mass fraction of the largest species were calculated from equations (5) and (6) using the newly calculated values for the remaining species. The process was repeated until convergence to a specified limit was achieved. There are at least three major deficiencies with this approach:

- (1) Extreme care must be used in specifying the initial mass fractions; otherwise, the iteration procedure diverges;
- (2) Near the stoichiometric point several of the species have mass fractions which are approximately equal. This causes different species to have the largest mass fraction in successive steps in the iteration procedure resulting in instability; and
- (3) A large amount of computer logic is required to handle the extreme variations in the input parameters resulting in relatively large computational times.

The continued use of the model and equations employed in reference [1] is recommended in this paper. However, a new solution procedure is proposed.

The remaining discussion defines the proposed new solution procedure and gives some results and conclusions regarding its application.

A.1 Derivation of Solution Procedure

The present procedure is based on the reduction of the number of variables under consideration. Two equations are derived as follows. Equations (13 - 16) are solved to give the relationships:

$$m_H = \frac{1}{\sqrt{K_1'}} \sqrt{m_{H_2}} \quad (17)$$

$$m_O = \frac{1}{\sqrt{K_2'}} \sqrt{m_{O_2}} \quad (18)$$

$$m_{H_2O} = \frac{K_3' K_4'}{K_1' \sqrt{K_2'}} m_{H_2} \sqrt{m_{O_2}} \quad (19)$$

$$m_{OH} = \frac{K_3'}{\sqrt{K_1' K_2'}} \sqrt{m_{H_2}} \sqrt{m_{O_2}} \quad (20)$$

It is convenient to define the following parameters:

$$\bar{A} = \frac{1}{\sqrt{K_1'}} \quad (21)$$

$$\bar{B} = \frac{1}{\sqrt{K_2'}} \quad (22)$$

$$\bar{C} = \frac{K_3' K_4'}{K_1' \sqrt{K_2'}} \quad (23)$$

$$\bar{D} = \frac{K_3'}{K_1' K_2'} \quad (24)$$

Using equations (17 - 20) to eliminate m_O , m_{H_2O} , m_H and m_{OH} from equations (5) and (6) gives:

$$X = m_{O_2} + \sqrt{m_{O_2}} \left[\bar{B} + \frac{8}{9} \bar{C} m_{H_2} + \frac{16}{17} \bar{D} \sqrt{m_{H_2}} \right] \quad (25)$$

$$F = m_{H_2} \left[1 + \frac{1}{9} \bar{C} m_{O_2} \right] + \sqrt{m_{H_2}} \left[\bar{A} + \frac{1}{17} \bar{D} m_{O_2} \right] \quad (26)$$

where the definitions given by equations (21 - 24) have been used. These equations have the form of a quadratic equation:

$$\bar{a}u^2 + \bar{b}u + \bar{c} = 0$$

and solution [3]

$$u = \frac{-2\bar{c}}{\bar{b} \pm \sqrt{\bar{b}^2 - 4\bar{a}\bar{c}}}$$

Note that \bar{a} and \bar{b} are always positive and \bar{c} is always negative. Since $u > 0$, the physically meaningful root is

$$u = \frac{-2\bar{c}}{\bar{b} + \sqrt{\bar{b}^2 - 4\bar{a}\bar{c}}} \quad (27)$$

This particular form of quadratic expression is chosen since it does not require subtraction and gives greater precision. Using equation (27) to express the solution of equations (25) and (26) gives

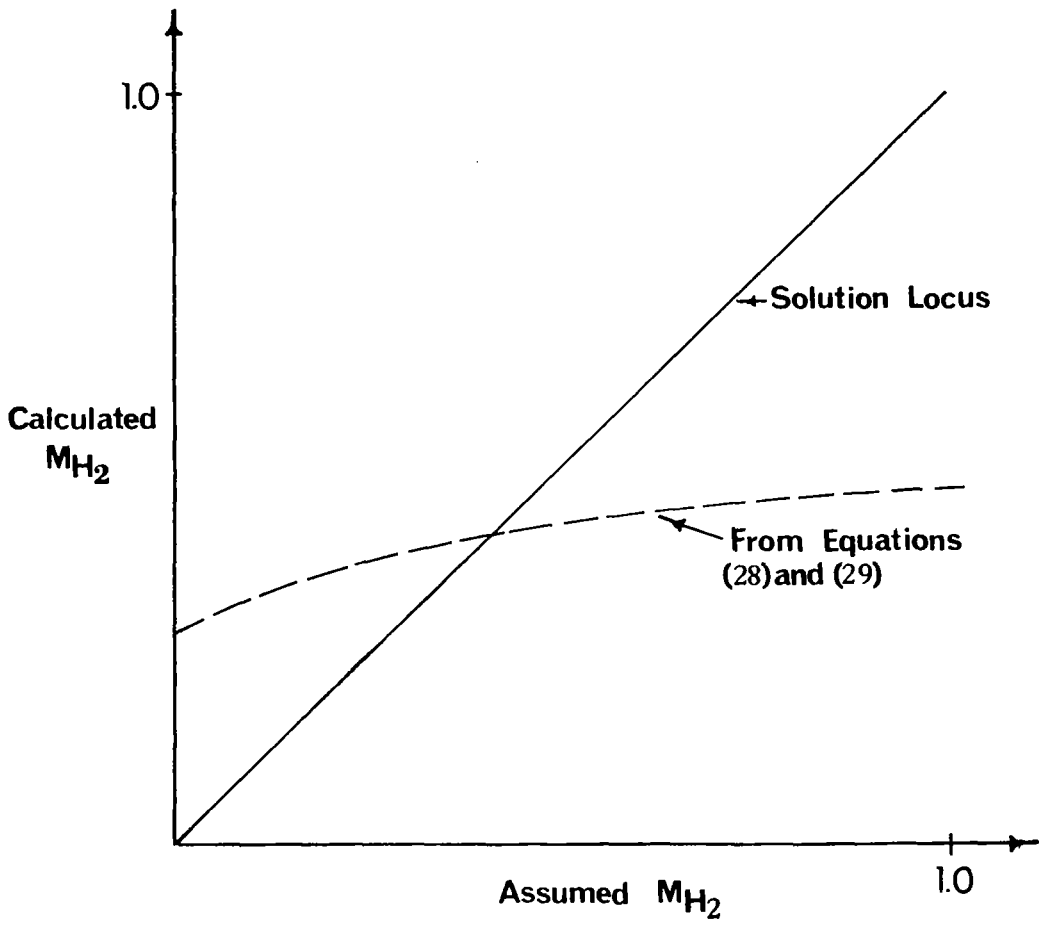
$$m_{O_2} = \frac{X}{\left[\frac{\bar{B} + \frac{8}{9} \bar{C} m_{H_2} + \frac{16}{17} \bar{D} \sqrt{m_{H_2}}}{2} \right] + \sqrt{\left(\frac{\bar{B} + \frac{8}{9} \bar{C} m_{H_2} + \frac{16}{17} \bar{D} \sqrt{m_{H_2}}}{2} \right)^2 + X}} \quad (28)$$

$$m_{H_2} = \frac{F}{\left[\frac{\bar{A} + \frac{1}{17} \bar{D} \sqrt{m_{O_2}}}{2} \right] + \sqrt{\left(\frac{\bar{A} + \frac{1}{17} \bar{D} \sqrt{m_{O_2}}}{2} \right)^2 + \left(1 + \frac{1}{9} \bar{C} \sqrt{m_{O_2}} \right) F}} \quad (29)$$

Equations (28) and (29) contain the unknowns m_{O_2} and m_{H_2} . Before detailing the solution procedure several properties of these equations will be discussed. Table I gives the values of K_1' , K_2' , K_3' , K_4' , \bar{A} , \bar{B} , \bar{C} , and \bar{D} for the temperatures from 100 to 6000 K at a constant PW product of 2.5 (corresponding approximately to 1/10 atmosphere). Note that while the individual constants vary from less than 1 to 10^{100} , the groups appearing in equations (28) and (29) vary much less and can be easily processed on a digital computer. Second it is to be observed that the equations have been derived so that a "natural" relationship has been established between m_{O_2} and X , and m_{H_2} and F , i.e. as $X \rightarrow 0$, $m_{O_2} \rightarrow 0$; and as $F \rightarrow 0$, $m_{H_2} \rightarrow 0$. It should also be observed that m_{O_2} and m_{H_2} can never be less than zero or greater than 1. Finally, neither equation becomes indefinite as m_{H_2} or m_{O_2} approach zero. Thus, the equations are well-behaved and can be readily solved for wide variations in temperature and pressure.

The solution procedure is described next. A value of m_{H_2} is guessed in the following way. If the value at the equivalent upstream station is known, then that value is used; otherwise, a value of zero will always lead to a converged solution. This assumed value of m_{H_2} is substituted into equation (28) which yields m_{O_2} . Then the computed value of m_{O_2} is substituted into equation (29) which allows calculation of a new value of m_{H_2} . The assumed and calculated values of m_{H_2} are compared. If their values differ by more than a specified convergence criteria, the calculated value of m_{H_2} is taken as the assumed value and the process described above is repeated until convergence is obtained. The behavior of this solution technique is shown in Figure A.1-1.

Figure I shows with the broken line a plot of m_{H_2} calculated versus m_{H_2} assumed. The correct value is achieved when the two values are equal. The locus of points for this situation is a straight line with a slope of unity. If m_{H_2} assumed is less than the correct value, the figure shows the calculated value will always be larger. Thus, when this calculated value of m_{H_2} is taken as the assumed value, the resulting newly calculated value will be closer to the correct one. The same argument can be made to show that if the initial assumed value of m_{H_2} is too large, the iteration process will again cause convergence to the correct value.



A.1-1. Graphical Plot of Trial-and-Error Solution

A.2 Typical Results

The solution procedure described above was programmed on a digital computer and used to determine equilibrium concentrations for variation in F and X from zero to one for temperatures from 200 to 5700 K. The product PW was taken at 2.5 (approximately 1/10 atmosphere pressure). Table II shows these calculated results. The residuals in F and X are shown in the last two columns. Their values indicate that great precision can be obtained with this method. The convergence criteria for these calculations was

$$|m_{H_2 \text{calculated}} - m_{H_2 \text{assumed}}| < .001 m_{H_2 \text{calculated}}$$

Greater precision could easily be achieved by a stricter convergence criteria; however, the present one is sufficient for most practical calculations.

It is concluded that the method offers a reliable, simple and extremely fast technique for solving the equilibrium equations arising from the chemical model considered in this work.

TABLE I.

Temp.	K_1	K_2	K_3	K_4	\bar{A}	\bar{B}	\bar{C}	\bar{D}
200	5.0+100	3.1E+99	2.6+100	2.6+100	4.4E-51	1.7E-50	2.1E+00	2.5E+50
400	2.8E+52	2.7E+58	3.2E+51	6.2E+59	5.9E-27	6.0E-30	1.1E-04	4.3E+29
600	2.3E+33	4.3E+36	5.8E+32	9.0E+37	2.0E-17	4.7E-19	5.7E-03	1.0E+19
800	5.9E+23	4.9E+25	2.2E+23	9.3E+26	1.2E-12	1.4E-13	4.0E-02	4.8E+13
1000	9.7E+17	1.2E+19	4.5E+17	2.2E+20	1.0E-09	2.7E-10	1.2E-01	2.8E+10
1200	1.2E+14	5.0E+14	7.0E+13	8.2E+15	8.7E-08	4.4E-08	2.7E-01	1.9E+08
1400	2.1E+11	3.5E+11	1.2E+11	5.4E+12	2.1E-06	1.6E-06	4.7E-01	5.5E+06
1600	1.7E+09	1.5E+09	1.1E+09	2.2E+10	2.4E-05	2.5E-05	7.0E-01	3.8E+05
1800	3.9E+07	2.1E+07	2.7E+07	3.0E+08	1.5E-04	2.1E-04	9.5E-01	4.6E+04
2000	1.9E+06	7.0E+05	1.4E+06	9.8E+06	7.2E-04	1.1E-03	1.2E+00	8.7E+03
2200	1.5E+05	4.3E+04	1.2E+05	5.8E+05	2.5E-03	4.8E-03	1.4E+00	2.2E+03
2400	1.9E+04	4.2E+03	1.6E+04	5.5E+04	7.0E-03	1.5E-02	1.7E+00	6.9E+02
2600	3.4E+03	5.8E+02	2.8E+03	7.6E+03	1.7E-02	4.1E-02	2.0E+00	2.6E+02
2800	7.5E+02	1.0E+02	6.4E+02	1.3E+03	3.6E-02	9.6E-02	2.2E+00	1.1E+02
3000	2.0E+02	2.4E+01	1.7E+02	3.1E+02	7.0E-02	2.0E-01	2.5E+00	5.5E+01
3200	6.3E+01	6.8E+00	5.7E+01	8.5E+01	1.2E-01	3.8E-01	2.7E+00	2.9E+01
3400	2.3E+01	2.1E+00	2.1E+01	2.7E+01	2.0E-01	6.7E-01	2.9E+00	1.6E+01
3600	9.3E+00	7.9E-01	8.6E+00	9.8E+00	3.2E-01	1.1E+00	3.1E+00	1.0E+01
3800	4.1E+00	3.2E-01	3.8E+00	3.9E+00	4.9E-01	1.7E+00	3.3E+00	6.5E+00
4000	1.9E+00	1.4E-01	1.8E+00	1.7E+00	7.0E-01	2.6E+00	3.5E+00	4.4E+00
4200	1.0E+00	6.8E-02	9.8E-01	8.3E-01	9.8E-01	3.8E+00	3.7E+00	3.0E+00
4400	5.5E-01	3.5E-02	5.4E-01	4.2E-01	1.3E+00	5.3E+00	3.8E+00	2.2E+00

TABLE I.
(Continued)

Temp.	K_1	K_2	K_3	K_4	\bar{A}	\bar{B}	\bar{C}	\bar{D}
4600	3.2E-01	1.8E-02	3.1E-01	2.2E-01	1.7E+00	7.2E+00	4.0E+00	1.6E+00
4800	1.9E-01	1.0E-02	1.9E-01	1.3E-01	2.2E+00	9.6E+00	4.1E+00	1.2E+00
5000	1.2E-01	6.4E-03	1.2E-01	7.7E-02	2.8E+00	1.2E+01	4.2E+00	9.5E-01
5200	7.9E-02	4.0E-03	7.8E-02	4.8E-02	3.5E+00	1.5E+01	4.4E+00	7.5E-01
5400	5.3E-02	2.5E-03	5.3E-02	3.1E-02	4.3E+00	1.9E+01	4.5E+00	6.0E-01
5600	3.6E-02	1.7E-03	3.6E-02	2.0E-02	5.2E+00	2.4E+01	4.6E+00	4.9E-01
5800	2.6E-02	1.1E-03	2.6E-02	1.4E-02	6.1E+00	2.9E+01	4.7E+00	4.1E-01
6000	1.8E-02	8.1E-04	1.8E-02	9.8E-03	7.2E+00	3.5E+01	4.8E+00	3.4E-01

TABLE II.

Temp.	F	X	m_{H_2}	m_{O_2}	m_H	m_O	m_{OH}	m_{H_2O}	RES ₁ *	RES ₂ **
200	0	.23200	.00000	.23200	0	0	0	.00000	-.00000	0
200	.2	.18560	.17677	.00000	0	0	0	.20903	-.00020	0
200	.4	.13920	.38259	.00000	0	0	0	.15665	-.00005	0
200	.6	.09280	.58840	.00000	0	0	0	.10441	-.00001	0
200	.8	.04640	.79419	.00000	0	0	0	.05228	-.00008	0
200	1.0	.00000	1.00000	.00000	0	0	0	.00001	-.00000	0
700	0	.23200	.00000	.23200	0	0	0	.00000	-.00000	0
700	.2	.18560	.17677	.00000	0	0	0	.20903	-.00020	0
700	.4	.13920	.38259	.00000	0	0	0	.15665	-.00005	0
700	.6	.09280	.58840	.00000	0	0	0	.10441	-.00001	0
700	.8	.04640	.79419	.00000	0	0	0	.05228	-.00008	0
700	1.0	.00000	1.00000	.00000	0	0	0	.00001	-.00000	0
1200	0	.23200	.00000	.23200	0	0	0	.00000	-.00000	0
1200	.2	.18560	.17677	.00000	0	0	0	.20903	-.00020	0
1200	.4	.13920	.38259	.00000	0	0	0	.15665	-.00005	0
1200	.6	.09280	.58840	.00000	0	0	0	.10441	-.00001	0
1200	.8	.04640	.79419	.00000	0	0	0	.05228	-.00008	0
1200	1.0	.00000	1.00000	.00000	0	0	0	.00001	-.00000	0
1700	0	.23200	.00000	.23196	.00000	.00004	0	.00000	-.00000	0
1700	.2	.18560	.17675	.00000	.00003	.00000	0	.20902	-.00020	0
1700	.4	.13920	.38255	.00000	.00004	.00000	0	.15665	-.00005	0

* Residual in F equation (29)

** Residual in X equation (28)

TABLE II.
(Continued)

Temp.	F	X	m_{H_2}	m_{O_2}	m_H	m_O	m_{OH}	m_{H_2O}	RES ₁ *	RES ₂ **
1700	.6	.09280	.58835	.00000	.00005	.00000	0	.10441	-.00001	0
1700	.8	.04640	.79413	.00000	.00006	.00000	0	.05228	-.00008	0
1700	1.0	.00000	.99993	.00000	.00007	.00000	0	.00000	-.00000	0
2200	0	.23200	.00000	.22970	.00000	.00230	.00000	.00000	-.00000	0
2200	.2	.18560	.17574	.00000	.00105	.00000	.00034	.20867	-.00020	0
2200	.4	.13920	.38106	.00000	.00155	.00000	.00017	.15647	-.00005	0
2200	.6	.09280	.58648	.00000	.00192	.00000	.00009	.10431	-.00001	0
2200	.8	.04640	.79196	.00000	.00223	.00000	.00004	.05224	-.00008	0
2200	1.0	.00000	.99749	.00000	.00251	.00000	.00000	.00000	-.00000	0
2700	0	.23200	.00000	.20310	.00000	.02890	.00000	.00000	-.00000	0
2700	.2	.18560	.16687	.00005	.01034	.00045	.00620	.20189	-.00019	0
2700	.4	.13920	.36746	.00001	.01534	.00016	.00317	.15311	-.00004	0
2700	.6	.09280	.56941	.00000	.01910	.00007	.00170	.10253	-.00001	0
2700	.8	.04640	.77200	.00000	.02223	.00002	.00073	.05148	-.00007	0
2700	1.0	.00000	.97501	.00000	.02499	.00000	.00000	.00000	-.00000	0
3200	0	.23200	.00000	.10689	.00000	.12511	.00000	.00000	-.00000	0
3200	.2	.18560	.13505	.00142	.04597	.01444	.03815	.15067	-.00011	0
3200	.4	.13920	.31439	.00019	.07014	.00527	.02124	.12800	-.00003	0
3200	.6	.09280	.50086	.00004	.08853	.00231	.01175	.08933	-.00001	0
3200	.8	.04640	.69065	.00001	.10395	.00086	.00514	.04586	-.00006	0
3200	1.0	.00000	.88249	.00000	.11751	.00000	.00000	.00000	-.00000	0

* Residual in F equation (29)

** Residual in X equation (28)

TABLE II.
(Continued)

Temp.	F	X	m_{H_2}	m_{O_2}	m_H	m_O	m_{OH}	m_{H_2O}	RES* ₁	RES** ₂
3700	0	.23200	.00000	.02210	.00000	.20990	.00000	.00000	-.00000	0
3700	.2	.18560	.07874	.00406	.11326	.08998	.05854	.04102	-.00000	0
3700	.4	.13920	.20737	.00102	.18380	.04514	.04766	.05420	-.00000	0
3700	.6	.09280	.35319	.00025	.23987	.02252	.03103	.04604	-.00010	0
3700	.8	.04640	.50841	.00004	.28779	.00897	.01483	.02640	-.00002	0
3700	1.0	.00000	.66970	.00000	.33030	.00000	.00000	.00000	-.00000	0
4200	0	.23200	.00000	.00357	.00000	.22843	.00000	.00000	-.00000	0
4200	.2	.18560	.02919	.00167	.16888	.15622	.02599	.00366	-.00000	0
4200	.4	.13920	.09410	.00072	.30323	.10272	.03068	.00775	-.00001	0
4200	.6	.09280	.35319	.00025	.23987	.02252	.03103	.04604	-.00010	0
4200	.8	.04640	.27764	.00005	.52084	.02758	.01415	.00614	-.00000	0
4200	1.0	.00000	.38593	.00000	.61407	.00000	.00000	.00000	-.00000	0
4700	0	.23200	.00000	.00076	.00000	.23124	.00000	.00000	0	0
4700	.2	.18560	.00904	.00045	.19045	.17716	.00824	.00027	0	0
4700	.4	.13920	.03336	.00023	.36589	.12760	.01140	.00072	0	0
4700	.6	.09280	.06985	.00010	.52942	.08188	.01059	.00097	0	0
4700	.8	.04640	.11632	.00002	.68320	.03949	.00659	.00078	0	0
4700	1.0	.00000	.17119	.00000	.82881	.00000	.00000	.00000	0	0
5200	0	.23200	.00000	.00022	.00000	.23178	.00000	.00000	0	0
5200	.2	.18560	.00308	.00013	.19675	.18278	.00283	.00003	0	0
5200	.4	.13920	.01195	.00007	.38780	.13517	.00413	.00008	0	0

* Residual in F equation (29)
** Residual in X equation (28)

TABLE II.
(Continued)

Temp.	F	X	m_{H_2}	m_{O_2}	m_H	m_O	m_{OH}	m_{H_2O}	RES ₁ *	RES ₂ **
5200	.6	.09280	.02615	.00003	.57360	.08889	.00402	.00011	0	0
5200	.8	.04640	.04526	.00001	.75458	.04385	.00261	.00009	0	0
5200	1.0	.00000	.06891	.00000	.93109	.00000	.00000	.00000	0	0
5700	0	.23200	.00000	.00008	.00000	.23192	.00000	.00000	0	0
5700	.2	.18560	.00122	.00005	.19871	.18448	.00113	.00000	0	0
5700	.4	.13920	.00483	.00003	.39507	.13758	.00168	.00001	0	0
5700	.6	.09280	.01075	.00001	.58916	.09121	.00166	.00002	0	0
5700	.8	.04640	.01889	.00000	.78105	.04535	.00109	.00001	0	0
5700	1.0	.00000	.02918	.00000	.97082	.00000	.00000	.00000	0	0

* Residual in F equation (29)

** Residual in X equation (28)

APPENDIX B

DEFINITION OF TERMS APPEARING IN COMMON STATEMENTS

AGEOM	factor in grid expansion defined in section 3.1
AK	mixing length constant, K
AKFAC	factor relating turbulence energy to mean motion energy
AMU	laminar viscosity, μ
AMUREF	reference laminar viscosity
AMUT	turbulent viscosity, μ_t
BXE	width of flow region along x-coordinate
BYN	width of flow region along y-coordinate
CD	constant in turbulence model, C_D
CDQR	C_D raised to 1/4 power
CDRT	C_D raised to 1/2 power
CDTQ	C_D raised to 3/4 power
CP	specific heat
CPDCV	specific heat at constant pressure divided by specific heat at constant volume
C1	constant in turbulence model, C_1
C2	constant in turbulence model, C_2
DEN	reference density
DZ	step length in z direction
EE	constant in law-of-the-wall, E
EX	factor by which forward step size is increased
FLOINJ	mass flow rate injected by a jet
FLUXN, FLUXS	flux of dependent variable at N and S boundaries respectively
FRA	fraction of boundary height used in calculating forward step
FRAM	maximum fraction of boundary layer height used in calculating forward step
FXM, FXP, FYM, FYP	interpolation factors to indicate distance of a pressure node from the neighboring velocity node
GAMN, GAMS	boundary value of GAM at N and S boundaries, respectively
GASCON	universal gas constant

GREAT	large number used in limiting overflows, etc.
H	recovery factor
HO	enthalpy of formation
IINJ	index to control entry to INJMOD
IMAX	maximum value of I for which storage locations are provided
INJSTP	value of ISTEP at injection location
INTEX	index: 1 for internal flows: 2 for external flows
IPRINT	values of a variable printed only if corresponding value of IPRINT is unity
IREF	reference value of I for printout
ISOLVE	equation for a variable is solved only if corresponding value of ISOLVE is unity
ISTEP	number of station
ISTR	value of I for the first storage location for a given variable
ISWP	index controlling direction if TDMA sweep along I coordinate
ITERF	counter for iterations on the ϕ equation
ITERM	counter for iteration on the momentum equation
IXY	index controlling the first direction of a TDMA sweep
JM	$(J - 1)JMAX$
JMAX	maximum value of J for which internal storage is provided
JSTR	value of J denoting the first internal storage location for a given variable
JSWP	index denoting the direction of sweep while performing TDMA sweep in y-direction
KBCN, KBCS	index denoting nature of N and S boundaries, respectively: 1 = wall; 2 = symmetry; 3 = free.
L	number of grid lines minus 1 in x-direction
LASTEP	number of station for which integration is to end
LCV	number of main control volumes in x-direction
LPI	number of grid lines in x-direction
M	number of grid lines minus 1 in y-direction
MCV	number of main control volumes in y-direction
MPI	number of grid lines in y-direction
NFM	number of variable $(NV)*IMAX*JMAX$

NFPMAX	maximum number of variables for which printout is arranged
NH	identifier of atomic hydrogen concentration
NH2	identifier of molecular hydrogen concentration
NH2O	identifier of water vapor concentration
MMU	identifier of viscosity
NNV	number of dependent variables
NN2	identifier of molecular nitrogen concentration
NO	identifier of atomic oxygen concentration
NOH	identifier of OH concentration
NO2	identifier of molecular oxygen concentration
NPJUMP	value equals ISTEP for printout of profile of variables
NPP	identifier of pressure correction
NRO	identifier of density
NSWP	number of TDMA sweeps on a variable
NV	serial number of any variable
NVD	identifier for dissipation rate of turbulence
NVF	identifier for hydrogen concentration in any form
NVH	identifier for enthalpy
NVK	identifier for turbulent kinetic energy
NVP	identifier for pressure
NVT	identifier for temperature
NVU	identifier for velocity in x-direction
NVV	identifier for velocity in y-direction
NVW	identifier for velocity in z-direction
PIN	inlet pressure
PJAY	resistance of laminar sublayer, P_ϕ
PR	Prandtl number, Pr
PRLAM	laminar Prandtl number/Schmidt number,
RETRAN	transition Reynolds number
SMALL	small number used to control underflows, etc.
TIN	inlet free stream temperature
TINJ	inlet jet temperature

TITLE	any title to describe calculations
TWAL	wall temperature
UIN	inlet x-direction velocity
VIN	inlet y-direction velocity
VINJ	velocity of jet injection
WIN	inlet free-stream velocity in z-direction
WM	molecular weight
X	x-coordinates
XDIF	distance between grid lines in x-direction
XS	width of main control volume in x-direction
XSU	width of u velocity control volume in x-direction
Y	y-coordinates
YDIF	distance between grid lines in y-direction
YS	width of main control volume in y-direction
YSV	width of v velocity control volume in y-direction
ZD	downstream location on control volume face in z-direction
ZETA	x/BXE
ZINJ	z location of injection
ZLAST	z location at end of integration
ZRE	values of z for which printout is desired
ZU	upstream location of control volume face in z-direction